การควบแน่นโบส-ไอน์สไตน์ของอะตอมไฮโดรเจน

นาย วัฒนา แซ่ลิ่ม

สถาบันวิทยบริการ
จุฬาลงกรณ์มหาวิทยาลัย

วิทยานิพนธ์นี้เป็นส่วนหนึ่งของการศึกษาตามหลักสูตรปริญญาวิทยาศาตรมหาบัณฑิต
สาขาวิชาฟิสิกส์ ภาควิชาฟิสิกส์
คณะวิทยาศาสตร์ จุฬาลงกรณ์มหาวิทยาลัย
ปีการศึกษา 2544

ISBN 974-17-0269-8

ลิขสิทธิ์ของจุฬาลงกรณ์มหาวิทยาลัย

BOSE-EINSTEIN CONDENSATION OF ATOMIC HYDROGEN

Mr. Wattana Lim

สถาบันวิทยบริการ
จุฬาลงกรณ์มหาวิทยาลัย

A Thesis Submitted in Partial Fulfillment of the Requirements
for the Degree of Master of Science in Physics

Department of Physics
Faculty of Science
Chulalongkorn University

Academic Year 2001
ISBN 974-17-0269-8

Thesis Title	Bose-Einstein Condensation of Atomic Hydrogen
By	Mr. Wattana Lim
Field of Study	Physics
Thesis Advisor	Professor Virulh Sa-yakanit, F.D.

Accepted by the Faculty of Science, Chulalongkorn University in Partial Fulfillment of the Requirements for the Master's Degree

..... Deputy Dean for Administrative Affairs

(Associate Professor Pipat Karntiang, Ph.D.) Acting Dean, Faculty of Science

THESIS COMMITTEE

..... Chairman

(Associate Professor Wichit Sritrakool, Ph.D.)

..... Thesis Advisor

(Professor Virulh Sa-yakanit, F.D.)

..... Member

(Rujikorn Dhanawittayapol, Ph.D.)

..... Member

(Sojiphong Chatraphorn, Ph.D.)

สถาบันวิทยบริการ
จุฬาลงกรณ์มหาวิทยาลัย

นาย วัฒนา แซ่ลิ่ม : การควบแน่นโบส-ไอน์สไตน์ของอะตอมไฮโดรเจน. (BOSE-EINSTEIN CONDENSATION OF ATOMIC HYDROGEN) อ. ที่ปรึกษา : ศ. ดร. วิรุฬห์ สายคณิต, 92 หน้า. ISBN 974-17-0269-8.

เราศึกษาสมบัติสถานะพื้นของการควบแน่นโบส-ไอน์สไตน์ของอะตอมไฮโดรเจนในสนามแม่เหล็กแบบ ออฟเฟ-พริทชาดร์ โดยทฤษฎีการอินทริเกรตเชิงเส้นแบบฟายน์แมนของอนุภาคหลายตัว ซึ่งนำไปสู่การคำนวณ พลังงานสถานะพื้น และฟังชันคลื่น เรายังคำนวณ ขนาด, ความหนาแน่นสูงของการควบแน่น และค่าของพลังงานสถานะพื้น ซึ่งมีค่าใกล้เคียงกับการทดลอง ซึ่งวัดโดยหลักการแยกความถี่แสงเลเซอร์ ของการเปลี่ยนระดับระหว่างสถานะ 1S กับ 2S

สถาบันวิทยบริการ
จุฬาลงกรณ์มหาวิทยาลัย

ภาควิชา ฟิสิกส์ ลายมือชื่อนิสิต.....
สาขาวิชา ฟิสิกส์ ลายมือชื่ออาจารย์ที่ปรึกษา.....
ปีการศึกษา 2544

4172438323 : MAJOR PHYSICS

KEY WORD: HYDROGEN / BEC / BOSE-EINSTEIN CONDENSATION / PATH INTEGRAL / GROUND STATE

WATTANA LIM: BOSE-EINSTEIN CONDENSATION OF ATOMIC HYDROGEN THESIS ADVISOR: PROF. VIRULH SA-YAKANIT, F.D., 92 pp. ISBN 974-17-0269-8.

We study the ground state properties of Bose-Einstein condensation of atomic hydrogen in the Ioffe-Pritchard magnetic trap using many-body Feynman Path Integral theory, which leads to the calculation of the ground state energy and the wave function. We also calculate the size, peak condensate density and the value of the ground state energy, which are in fair agreement with the experimental results obtained by laser spectroscopy of 1S-2S transition.

สถาบันวิทยบริการ
จุฬาลงกรณ์มหาวิทยาลัย

Department Physics Student's signature.....

Field of study Physics Advisor's signature.....

Academic year 2001

Acknowledgements

I wish to express my deep gratitude to my supervisor, Prof. Dr. Virulh Sa-yakanit for his advice, guidance and encouragement throughout the course of this thesis. I am grateful to him for allowing me to work in his research group (FTS) and for supporting me in various ways. The next important person to whom I want to express my thanks is Dr. Rujikorn Dhanawittayapol for giving his valuable time in the discussion of the problem of my thesis. I also would like to thank Mr. Kobchai Tayanasanti for his valuable advice. Finally, I wish to thank Miss Khattiya Chalapat for her assistance in typing this thesis in the LaTeX format.

สถาบันวิทยบริการ
จุฬาลงกรณ์มหาวิทยาลัย

Contents

สถาบันวิทยบริการ
จุฬาลงกรณ์มหาวิทยาลัย

List of Tables

สถาบันวิทยบริการ
จุฬาลงกรณ์มหาวิทยาลัย

List of Figures

สถาบันวิทยบริการ
จุฬาลงกรณ์มหาวิทยาลัย

Chapter 1
Introduction

The phenomenon of Bose-Einstein condensation was predicted by S.N. Bose and A. Einstein in 1924 [1], during the early days of quantum mechanics. They studied the statistical properties of massive particles with integer spins, which are known as bosons. It was found that not only it is possible for two or more bosons to share the same quantum state, but also the bosons actually prefer being in the same state. It was predicted that at a finite temperature, almost all the particles of a bosonic system would occupy the ground state as soon as the quantum wave functions of the particles start to overlap. In a Bose-Einstein condensate millions of atoms occupy a single quantum state, thus bringing the quantum world into the macroscopic regime.

In the 1930, Fritz London investigated superfluidity in liquid helium. From the very beginning he realized that superfluidity could be a manifestation of Bose-Einstein condensation. However, due to the strong interaction between the helium atoms, the analyses have remained unsatisfactory.

After the huge success of the cooling atoms by laser light, a method proposed by T.W. Hänsch and A. Schalow in 1975, researchers investigated the possibility of producing a Bose-Einstein condensate using alkali atoms. In the summer of 1995, BEC was reported by scientists at JILA (Boulder) [2], followed by similar reports from Rice University (Texas) [3], MIT (Cambridge) [4], the MPQ (Max-Planck Institute of quantum optics) group and the University of Munich. The breakthrough was made possible by combining laser cooling with evaporative cooling in a magnetic trap. The first evidence for condensation emerged from time

of flight measurements. A sharp peak in the velocity distribution was observed below a critical temperature.

In 1978 Thomas Greytak and Daniel Kleppner, leaders of a group at the Massachusetts Institute of Technology, started intensive efforts to form BECs in dilute hydrogen gases [5]. Twenty years later (in June 1998) they finally reached their goal by using dilution refrigerators, magnetic trapping and evaporative cooling. Hydrogen is a very interesting element to study BEC, because its small scattering length makes it an almost ideal Bose gas. Furthermore a hydrogen atom is generally appealing for basic studies because its structure and interactions can be calculated from the first principle and should allow for more precise comparisons with theories.

1.1 Hydrogen is Different

Hydrogen differs in several ways from alkali metal atoms that have been Bose condensed. The principal differences are its small mass and small s-wave scattering length as shown in Table 1.1. How do these properties influence the system? First, the small mass implies that BEC should occurs at a higher temperature. The transition temperatures is roughly 50 times higher than in other systems. Further, thermal equilibrium must be balanced by heating and evaporative cooling. For hydrogen the equilibrium condensate fraction is small because the high condensate density leads to high losses through dipolar decay, which results in heating of the system. Finally, hydrogen has small collision cross-section, which should allow condensates of H to be produced by evaporative cooling that contains many orders of magnitude more atoms than those possible in alkali-metal species.

Elements	H	Li	Na	Rb
Mass (amu)	1	7	23	87
BEC transition temperature (μK)	60	0.3	2	0.67
S-wave scattering length (Å)	0.648	-14.4	27.5	57.1
Peak condensate (cm^3)	5×10^{15}	2×10^{13}	3×10^{15}	5×10^{14}
Collision cross section	1×10^{-15}	5×10^{-13}	2×10^{-12}	8×10^{-12}
Dilutivity, $an_p^{1/3}$	1×10^{-3}	4×10^{-3}	4×10^{-2}	5×10^{-2}

Table 1.1: Comparison of the the parameters of alkali metal atoms [2].

1.2 The Organization of the Thesis

This thesis is organized as follows. Chapter 2 provides a detailed description of the trapped gas and a review of the concept of path integral theory. Chapter 3 describes the experiment on BEC in hydrogen. I will explain a technique of probing Bose condensates, optical spectroscopy. Using this tool, one can measure the density and momentum distributions of the sample, and thus infers the temperature, size of the condensate, and other properties. Chapter 4 describes the ground state properties of atomic hydrogen, using many-body Feynman 's path integral theory. I also calculate the expression of ground state energy and its wave function. Chapter 5 provides interpretation of the meaning of the results from Chapter 4. I minimized the expression of ground state energy by a numerical method that yields the values of ground state energy, size of the condensate, peak condensate density and other properties. I found that the results are in good agreement with the experiment. Finally, conclusion and discussion are drawn in Chapter 6.

สถาบันวิทยบริการ
จุฬาลงกรณ์มหาวิทยาลัย

Chapter 2
Theoretical Reviews

In this chapter I will review the basic concepts of BEC, which are used in this thesis. I also describe the occurrence of BEC and description of the condensate. Finally, I will briftly discuss the concepts of Feynman's path integral theory.

2.1 Degenerate Bose gas

2.1.1 Bose Distribution

The statistical mechanical description of classical gas is not correct when the temperature approach to zero. A simple way to understand the crossover to the quantum regime is to recall that particles are characterized by wavepackets whose sizes are related to their momenta by Heisenberg's momentum-position uncertainty relation. The thermal de Broglie wavelength is defined as

$$\lambda = \sqrt{\frac{2\pi\hbar^2}{k_B T m}} \tag{2.1}$$

where $\hbar$ and k_B are Planck's constant and Boltzmann's constant respectively, and m is the mass of the particle.

As the gas is cooled, the particle momenta decrease, and wavepackets become larger. The classical description of the system breaks down when the these wavepackets begin to overlap. The quantum treatment thus deals with the effect of the particle indistinguishability.

Here I review the basic features that are important for this thesis. The occupation function for gas of N identical bosons in a box of volume V, and in the limit of $N \to \infty$ and $V \to \infty$ but N/V is finite, is called the Bose-Einstein occupation function [6]

$$\overline{n}(\varepsilon) = \frac{1}{e^{(\varepsilon-\mu)/k_B T} - 1}, \tag{2.2}$$

where μ and T are Lagrange multipliers which constrain the system to exhibit the correct population and total energy through the conditions

$$\frac{N}{V} = \int d\varepsilon \frac{\rho(\varepsilon)}{V} \overline{n}(\varepsilon) \tag{2.3}$$

and

$$\frac{E}{V} = \int d\varepsilon \frac{\rho(\varepsilon)}{V} \varepsilon \overline{n}(\varepsilon) \tag{2.4}$$

respectively, where $\rho(\varepsilon)$ is total energy density of state function. The physical interpretaion of these parameter is that μ is the chemical potential and T is the temperature. The energy distribution of the population in the trap for a classical gas is described by the Maxwell-Boltzmann distribution and for a quantum gas is described by the Bose-Einstein distribution. Bose-Einstein condensation occurs when the chemical potential goes to zero and the occupation of the lowest energy state diverges. This occurs at the critical density [6]

$$n_c = g_{3/2}(1)\lambda^3(T) \tag{2.5}$$

where $g_n(z) \equiv \sum_{l=1}^{\infty} \frac{z^l}{l^n}$; $g_{3/2}(1) = 2.612$. A gas that has undergone the Bose-Einstein phase transition is said to be in the quantum degenerate regime because a macroscopic fraction of the particles are in an identical quantum state.

Although a hydrogen atom consists of two fermions, it behaves like a composite boson for the studies in this thesis because the collision interaction

energies are extremely small compared to the electron-proton binding energy [7]. The two fermions acts as a unit except in high energy collisions when electron exchange is possible. The typical interaction energy during low temperature collision is ~ 1 mK, which corresponds to 10^{-7} eV, 10^{8} times smaller than the binding energy.

2.2 Description of the Condensate

2.2.1 Gross-Pitaevskii Equation

When Bose-Einstein condensation occurs, a macroscopic fraction of the particles occupy the lowest energy quantum state of the system, and thus have the same wave functions. For a non-interacting Bose gas, that wave function is simply the lowest harmonic oscillator wave function for the harmonic trap. Interactions become important when many particles occupy the condensation in space and the local density increases. In this case the wavefunction spreads out due to the repulsion among of the atoms.

The Schrödinger equation for the interacting condensate is called the Gross-Pitaevskii equation [1], and has the form

$$-\frac{\hbar^2}{2m}\nabla^2\psi(\mathbf{r}) + V(\mathbf{r})\psi(\mathbf{r}) + U_0\left|\psi(\mathbf{r})\right|^2\psi(\mathbf{r}) = \mu\psi(\mathbf{r}) \tag{2.6}$$

where $\psi(\mathbf{r})$ is the condensate wavefunction. The eigenenergy of the wavefunction is μ, which is the total energy of each condensate atom. The quantity $U_0 = 4\pi\hbar^2 a/m$ is the mean field energy, which is the energy of interaction among the atoms per unit density, which is repulsive for s-wave scattering length $a > 0$. For a hydrogen atom in its ground state, $a = 0.648$ Å [8], and $U_0/k_B = 3.92$ 10^{-16} μKcm^3. The mean field energy augments the trap potential by an amount

proportional to the local condensate density $n_{cond}(\mathbf{r}) = |\psi(\mathbf{r})|^2$. It should note here that the interaction between the condensate and non-condensate atoms are neglected here. The eigenenergy μ in Eq. (2.6) and μ in Eq. (2.2) are the chemical potential of the system in equilibrium. The chemical potential is the energy required to add a particle to the system. When a condensate is present, the normal gas is saturated, and any particles added to the system go into the condensate. The energy required to add the last atom to the condensate is μ, and so I relate μ with the chemical potential. In some experiments μ is measured spectroscopically through the peak density at the center of the condensate, which is in turn measured through the cold-collision frequency shift [5].

2.2.2 Thomas-Fermi Approximation

When Bose-Einstein condensation occurs, many atoms occupy the lowest energy quantum state, the kinetic energy approaches to zero, then the kinetic energy term in Eq.(2.6) may be neglected. This leads to the Thomas-Fermi wave function

$$\psi(\mathbf{r}) = \begin{cases} N^{-1/2}\left[n_p - V\left(\mathbf{r}\right)/U_0\right]^{1/2} & V\left(\mathbf{r}\right) \leq n_p U_0 \\ 0 & \text{elsewhere} \end{cases} \tag{2.7}$$

where $n_p = \mu(N)/U_0$ is the peak condensate density and $V(\mathbf{r})$ is the potential energy. Here, $n_{cond}(\mathbf{r}) = N\left|\psi(\mathbf{r})\right|^2$ is the density distribution in the N-particle condensate. One can interpret $|\psi(\mathbf{r}_i)|^2$ as the probability of finding condensate particle particle i at position $\mathbf{r}_i$. Therefore we obtain the condensate density profile.

$$n_{cond}(\mathbf{r}) = n_p - V(\mathbf{r})/U_0 \tag{2.8}$$

The Thomas-Fermi approximation is valid over most of the volume of the condensate, but at near the edges the condensate density approaches zero, and kinetic energy term should be included.

The condensate density profile may be obtained without the Gross-Pitaevskii equation by assuming that the condensate is stationary and its particles are at rest, and then balancing hydrodynamic forces. A condensate particle in a region of the potential energy ε has total energy $E = \varepsilon + n_{cond}(\varepsilon) U_0$. Since there must be no net force on the particle, on the particle, $E = const \equiv n_p U_0$ and $n_{cond}(\varepsilon) = n_p - \varepsilon/U_0$.

2.3 Feynman's Path Integral Theory

In classical mechanics, the principle of the least action is a way of expressing the condition that determines the particular path $\overline{x}(t)$ out of all the possible paths. That is, there exists a certain quantity S which can be computed for each path. The classical path $\overline{x}(t)$ is the path that S is extremum. So the value of S is unchanged in the first order if the path $\overline{x}(t)$ is modified slightly from the classical path. The quantity S is given by the expression [9]

$$S = \int_{t_a}^{t_b} L(\dot{x}, x, t) dt, \tag{2.9}$$

where L is the lagrangian for the system. For a particle of mass m moving in a potential $V(x,t)$, which is a function of position and time the lagrangian is $L = \frac{m}{2}\dot{x}^2 - V(x,t)$.

In quantum-mechanical, we can not exactly know in which paths the particle go from a to b. Consequently, the total amplitude to go from a to b must be contributed by all path. Feynman found that they contribute equal amounts to the total amplitude, but contribute at different phases. The phase of the contribution from a given path equal to $S/\hbar$.

The probability $P(b,a)$ to go from x_a at the time t_a to x_b at the time t_b can be calculated as follow:

$$P(b,a) = |K(b,a)|^2 \tag{2.10}$$

where $K(b,a)$ is an amplitude to go from a to b. This amplitude is the sum of contribution $\phi[x(t)]$ from each path

$$K(b,a) = \sum_{\text{over all paths from a to b}} \phi[x(t)], \tag{2.11}$$

where

$$\phi[x(t)] = (const) \exp\left[\frac{i}{\hbar} S\{x(t)\}\right]. \tag{2.12}$$

The action S is that for the corresponding classical system. The constant will be chosen to normalize K conveniently.

Constructing the sum.

One choose a subset of all paths by first dividing the time intervals into small interval, ϵ. This gives a set of successive times $t_1, t_2, t_3, \ldots$ between the values t_a and t_b, where $t_{i+1} = t_i + \epsilon$. At each time, t_i, one select some special point x_i and construct a path by connecting all of the successive points by straight line. This processes are shown in Figure 2.1. It is possible to define a sum over all paths constructed in this manner by taking a multiple integral over all values of x_i for i from 1 to $n-1$, where

$$\begin{aligned} N\epsilon &= t_b - t_a \\ \epsilon &= t_{i+1} - t_i \\ t_0 &= t_a \ , \quad t_N = t_b \\ x_0 &= x_a \ , \quad x_N = x_b \end{aligned} \tag{2.13}$$

สถาบันวิทยบริการ
จุฬาลงกรณ์มหาวิทยาลัย

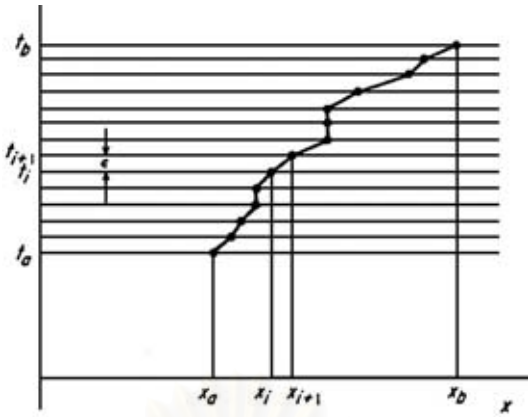

Figure 2.1: Diagram showing the sum over paths defined as a limit, in which at first the path is specified by giving only its coordinate x at a large number of specified times separated by very small intervals ϵ [1].

The resulting equation is

$$K(b,a) = \int\int\ldots\int (const) \exp\left[\frac{i}{\hbar} S\{x(t)\}\right] dx_1 dx_2 \ldots dx_{n-1} \tag{2.14}$$

We do not integrate x_0 or x_n because these are the fixed end point x_a and x_b. In order to achieve the correct measure, Eq. (2.14) must be taken in the limit of $\epsilon \to 0$ and some normalizing factor A^{-n} which depends on ϵ must be provided in order that the limit of Eq.(2.14) becomes

$$K(b,a) \approx \lim_{\epsilon\to 0} \frac{1}{A} \int\int\ldots\int (const) \exp\left[\frac{i}{\hbar} S\{x(t)\}\right] \frac{dx_1}{A}\frac{dx_2}{A}\ldots\frac{dx_n}{A} \tag{2.15}$$

This equation can also be written in a less restrictive notation as

$$K(b,a) \approx N \int\int\ldots\int (const) \exp\left[\frac{i}{\hbar} S\{x(t)\}\right] \mathcal{D}(\text{path}) \tag{2.16}$$

This is called a path integral and the amplitude $K(b,a)$ is known as the Feynman propagator or the kernel.

Harmonic oscillator

We consider the one dimensional harmonic oscillator described by the Lagrangian

$$L = \frac{1}{2}m\dot{x}^2 - \frac{1}{2}m\omega^2 x^2. \tag{2.17}$$

Thus the kernel can be written as

$$K(b,a) = \int_{x_2}^{x_2} \exp\left[\frac{i}{\hbar}\int_0^T \left(\frac{1}{2}m\dot{x}^2 - \frac{1}{2}m\omega^2 x^2\right) dt\right] \mathcal{D}x(t), \tag{2.18}$$

the integral over all paths which go from $(x_1, 0)$ to (x_2, T)

In classical mechanics, the form of the action integral $S = \int L dt$ is interesting, not just the extreme value S_{cl}. This interest derives from the necessity to know the action along a set of the neighboring paths in order to determine the path of the least action which the following condition is always satisfied:

$$\frac{d}{dt}\left(\frac{\partial L}{\partial \dot{x}}\right) - \frac{\partial L}{\partial \overline{x}} = 0. \tag{2.19}$$

For a harmonic oscillator, we can write Eq. (2.19) as

$$\ddot{\overline{x}} + \omega^2 \overline{x} = 0. \tag{2.20}$$

The solution of Eq. (2.20) is

$$\overline{x}(t) = A\sin\omega t + B\cos\omega t \tag{2.21}$$

where A and B are constants. By applying the boundary conditions $\overline{x}(0) = x_1$ and $\overline{x}(T) = x_2$ to Eq. (2.21), we can obtain the constant A and B,

$$\begin{aligned} A &= \frac{x_2 - x_1\cos\omega T}{\sin\omega T}, \\ B &= x_1. \end{aligned} \tag{2.22}$$

Now

$$\begin{aligned} S_{cl} &= \int_0^T \frac{m}{2}\left(\dot{\overline{x}}(t) - \omega\overline{x}(t)^2\right) dt \\ &= \frac{m}{2}\left[\dot{\overline{x}}(t)\overline{x}(t)\Big|_0^T - \int_0^T \overline{x}(t)\ddot{\overline{x}}(t)dt - \omega^2\int_0^T \overline{x}(t)^2 dt\right] \\ &= \frac{m}{2}\left[\dot{\overline{x}}(T)\overline{x}(T) - \dot{\overline{x}}(0)\overline{x}(0) - \int_0^T \overline{x}\left(\ddot{\overline{x}}(t) - \omega^2\overline{x}(t)\right) dt\right]. \end{aligned} \tag{2.23}$$

We find that the second term of Eq. (2.23) is equal to zero, so we obtain

$$S_{cl} = \frac{m}{2}\left[\dot{\overline{x}}(T)\overline{x}(T) - \dot{\overline{x}}(0)\overline{x}(0)\right]. \tag{2.24}$$

Differentiating Eq. (2.21) with respect to t, we obtain

$$\overline{x}(t) = A\omega\sin\omega t - B\omega\cos\omega t. \tag{2.25}$$

Substituting Eqs. (2.21), (2.25) and (2.22) into Eq. (2.24), we can write the classical action of the harmonic oscillator as

$$S_{cl} = \frac{m\omega}{2\sin\omega T}\left[\cos\omega T(x_1^2 + x_2^2) - 2x_1x_2\right]. \tag{2.26}$$

Let $\overline{x}(t)$ be the classical path between the specified end points. This is the path which is an extremum for the action S. In the notation we have been using

$$S_{cl}[x_2, x_1] = S[\overline{x}(t)]. \tag{2.27}$$

We can represent x in terms of $\overline{x}$ and a new variable y by

$$x(t) = \overline{x}(t) + y(t). \tag{2.28}$$

This is to say, instead of defining a point on the path by its distance $x(t)$ from an arbitrary coordinate axis, we measure in stead the deviation $y(t)$ from the classical path, as shown in Fiq. 2.2. Thus, we can write the action as

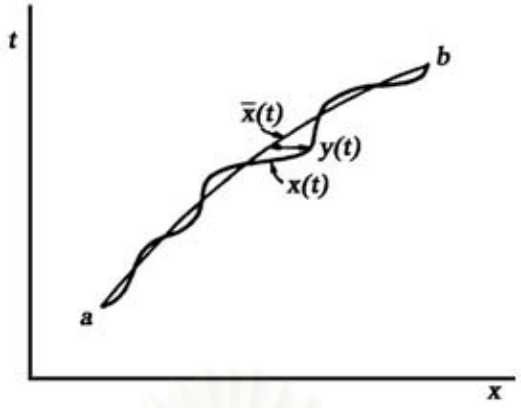

Figure 2.2: The difference between the classical path $\overline{x}(t)$ and some possible alternative path $x(t)$ is the function $y(t)$ [1].

$$\begin{aligned} S\left[x(t)\right] &= \int_0^T \left\{ \frac{m}{2}\left[\dot{\overline{x}}(t)+\dot{y}(t)\right]^2 - \frac{m\omega^2}{2}\left[\overline{x}(t)+y(t)\right]^2 \right\} dt \\ &= \int_0^T \left(\begin{array}{c} \frac{m}{2}\left[\dot{\overline{x}}^2(t)+2\,\dot{\overline{x}}\,(t)\dot{y}(t)+\dot{y}^2(t)\right] \\ -\frac{m\omega^2}{2}\left[\overline{x}^2(t)+2\overline{x}^2(t)y^2(t)+y^2(t)\right] \end{array} \right) dt \end{aligned} \tag{2.29}$$

or

$$S\left[x(t)\right] = S_{cl}\left[\overline{x}(t)\right] + \int_0^T \left[\frac{m}{2}\,\dot{y}^2\,(t) - \frac{m\omega^2}{2} y^2(t) \right] dt. \tag{2.30}$$

Substituting Eq. (2.30) into Eq. (2.18), we obtain

$$K(b,a) = \exp\left\{ \frac{i}{\hbar} S_{cl}\left[\overline{x}(t)\right] \right\} \int_0^0 \exp\left\{ \frac{i}{\hbar} \int_0^T \left[\frac{m}{2}\dot{y}^2(t) - \frac{m\omega^2}{2} y^2(t) \right] dt \right\} \mathcal{D}(y(t)) \tag{2.31}$$

We find that the integral over $y(t)$ does not depend on the classical path and $y(t) = 0$ at t_{x_1} and t_{x_2} so we use symbol $\int_0^0$ for integrate closed contour. We may write the kernel as

$$K(b,a) = F(T,0) \exp\left\{ \frac{i}{\hbar} S_{cl}\left[\overline{x}(t)\right] \right\} \tag{2.32}$$

where

$$F(T,0)=\int_0^0 \exp\left\{\frac{i}{\hbar}\int_0^T\left[\frac{m}{2}\,\dot{y}^2\,(t)-\frac{m\omega^2}{2}y^2(t)\right]dt\right\}\mathcal{D}(y(t)). \tag{2.33}$$

We can calculate $F(T,0)$ by expanding $y(t)$ as a Fourier series

$$y(t)=\sum_n a_n \sin\frac{n\pi t}{T} \tag{2.34}$$

and then consider the paths as a function of the coefficient a_n instead of functions of $y(t)$. The details for calculating $F(T,0)$ is given by Feyman and Hibbs. The result is

$$F(T)=\left(\frac{m\omega}{2\pi i\hbar\sin\omega T}\right)^{1/2}. \tag{2.35}$$

Therefore the kernel of harmonic oscillator is

$$K(b,a)=\left(\frac{m\omega}{2\pi i\hbar\sin\omega T}\right)^{1/2}\exp\left[\frac{im\omega}{2\hbar\sin\omega T}\left[\cos\omega T(x_1^2+x_2^2)-2x_1x_2\right]\right]. \tag{2.36}$$

This kernel can be expanded in exponential function. That is,

$$\begin{aligned}&\left(\frac{m\omega}{2\pi i\hbar\sin\omega T}\right)^{1/2}\exp\left[\frac{im\omega}{2\hbar\sin\omega T}\left[\cos\omega T(x_1^2+x_2^2)-2x_1x_2\right]\right]\\ =\;&\sum_{n=o}^{\infty}e^{-(i/\hbar)E_nT}\phi_n(x_2)\phi_n^*(x_1),\end{aligned} \tag{2.37}$$

where $\phi_n(x)$ is wave function and E_n is energy levels for $n=0,1,2,....$ Using the relations

$$\begin{aligned}(i\sin\omega T)^{-1} &= \frac{2e^{-i\omega T}}{(1-e^{-2i\omega T})}\\ (\cos\omega T)^{-1} &= \frac{2e^{-i\omega T}}{(1+e^{-2i\omega T})}\end{aligned} \tag{2.38}$$

We can write the left-hand side of Eq. (2.37) as

$$\begin{aligned}&\left(\frac{m\omega}{\pi\hbar}\right)^{1/2}e^{-i\omega T/2}(1-e^{-2i\omega T})^{-1/2}\\ &\times\exp\left\{-\frac{m\omega}{\pi\hbar}\left[(x_1^2+x_2^2)\left(\frac{1+e^{-2i\omega T}}{1-e^{-2i\omega T}}\right)-\frac{4x_1x_2e^{-i\omega T}}{1-e^{-2i\omega T}}\right]\right\}\end{aligned} \tag{2.39}$$

We can obtain a series having the form of the right-hand side of Eq. (2.37) in successive power of $e^{-i\omega T}$. Because of the initial factor $e^{-i\omega T/2}$, it is clear that all terms in the exponential will be of the form $e^{-i\omega T/2}e^{-in\omega T}$ for $n = 0, 1, 2, ...$ This means the energy levels are given by $E_n = \hbar\omega(n + 1/2)$.

To find the wave functions, we shall have to carry out the expansion completely. We shall illustrate the method by going only as far as $n = 2$. Expanding the left-hand side of Eq. (2.37) to this order we have

$$\left(\frac{m\omega}{\pi\hbar}\right)^{1/2} e^{-i\omega T/2}(1 + \frac{1}{2}e^{-2i\omega T} + ...) \\ \times \exp\left[-\frac{m\omega}{2\hbar}(x_1^2 + x_2^2) - \frac{m\omega}{\hbar}(x_1^2 + x_2^2)(e^{-2i\omega T} + ...) + \frac{2m\omega}{\hbar}x_1x_2e^{-i\omega T} + ...\right] \tag{2.40}$$

or

$$\left(\frac{m\omega}{\pi\hbar}\right)^{1/2} e^{-\frac{m\omega}{2\hbar}(x_1^2+x_2^2)}e^{-i\omega T/2}(1 + \frac{1}{2}e^{-2i\omega T} + ...) \\ \times \left[1 + \frac{2m\omega}{\hbar}x_1x_2e^{-i\omega T} + \frac{2m^2\omega^2}{\hbar^2}x_1^2x_2^2e^{-2i\omega T} - \frac{m\omega}{\hbar}(x_1^2 + x_2^2)e^{-2i\omega T} + ...\right]. \tag{2.41}$$

From this we pick out the coefficient of the lowest term. It is

$$\left(\frac{m\omega}{\pi\hbar}\right)^{1/2} e^{-\frac{m\omega}{2\hbar}(x_1^2+x_2^2)}e^{-i\omega T/2} = e^{-(i/\hbar)E_0T}\phi_0(x_2)\phi_0^*(x_1). \tag{2.42}$$

This mean that $E_0 = \frac{1}{2}\hbar\omega$ and

$$\phi_0(x) = \left(\frac{m\omega}{\pi\hbar}\right)^{1/4} e^{-(m\omega x^2/2\hbar)}. \tag{2.43}$$

The next-order term in the expansion is

$$e^{-i\omega T/2}e^{-i\omega T/}\frac{m\omega}{\pi\hbar}e^{-\frac{m\omega}{2\hbar}(x_1^2+x_2^2)}\frac{2m\omega}{\hbar} = e^{-(i/\hbar)E_1T}\phi_1(x_2)\phi_1^*(x_1) \tag{2.44}$$

which implies that $E_1 = \frac{3}{2}\hbar\omega$, and

$$\phi_1(x) = \frac{2m\omega}{\hbar}\phi_0(x). \tag{2.45}$$

The next term corresponds to $E_2 = \frac{5}{2}\hbar\omega$. The part of the term depending on x_1 and x_2 is

$$\left(\frac{m\omega}{\pi\hbar}\right)^{1/2} e^{-\frac{m\omega}{2\hbar}(x_1^2+x_2^2)} \left[\frac{2m^2\omega^2}{\hbar^2}x_1^2x_2^2 - \frac{m\omega}{\hbar}(x_1^2+x_2^2) + \frac{1}{2}\right]. \tag{2.46}$$

This must be the same as $\phi_2(x_2)\phi_2^*(x_1)$. Since the expression in the brackets can be re written as

$$\frac{1}{2}\left(\frac{2m\omega}{\hbar}x_1^2 - 1\right)\left(\frac{2m\omega}{\hbar}x_2^2 - 1\right) \tag{2.47}$$

we find

$$\phi_2(x) = \frac{1}{\sqrt{2}}\left(\frac{2m\omega}{\hbar}x^2 - 1\right)\phi_0(x). \tag{2.48}$$

All wave functions may be obtained in this manner. However, it is a difficult algebraic problem to get the general from for $\phi_n(x)$ directly from this expansion. From these results, we obtain the energy levels of the harmonic oscillator,

$$E_n = \hbar\omega(n + \frac{1}{2}) \tag{2.49}$$

where n is an integer 0,1,2.... and all of the wave functions can be written in the term of Hermite polynomials [9],

$$\phi_n = (2^n n!)\left(\frac{m\omega}{\pi\hbar}\right) H_n\left(x\sqrt{\frac{m\omega}{\hbar}}\right) e^{-(m\omega x^2/2\hbar)}. \tag{2.50}$$

Therefore we can obtain energy levels and wave functions from the kernel of the harmonic oscillator. This chapter I have described basic concepts of BEC for ideal Bose gas. I also described BEC for interacting Bose gas, which is described by Gross-Pitaevskii equation and Thomas-Fermi approximation. These concepts

allow us to understand the behavior of the trapped gas. Finally I discussed the concepts of Feynman path integral theory. I will use this concept to find the ground energy and the wave function of hydrogen condensate. This will be done in Chapter 4.

สถาบันวิทยบริการ
จุฬาลงกรณ์มหาวิทยาลัย

Chapter 3

Experiment on Bose-Einstein Condensation of Atomic Hydrogen

Bose-Einstein condensation (BEC) in hydrogen was observed for the first time by MIT (Massachusetts Institute of Technology) research group in 1998 [5]. However, the search for BEC in hydrogen began in 1976 [10]. Originally they polarized the gas by letting it flow into a strong magnetic field that attracted atoms with spins oriented antiparallel to the field and repelled the others. However the group found that with this method they could not reach the extremely low temperatures needed for a BEC because of collisions with the walls of the container. They solved this problem by reconfiguring the field to be weaker in the center, so that atoms with spins parallel to the field collected there, in a magnetic trap. Gradually reducing the field strength at the edge of the trap made it shallower and allowed higher energy atoms to escape. This method was called evaporative cooling. To reach their goal, the MIT group added a final cooling step by applying a radio frequency magnetic field that tuned to flip the spins of the most energetic hydrogen atoms, for this reason they were immediately attracted to the outer, stronger-field regions. Finally, the gas was cooled into the quantum degenerate regime. The hydrogen condensates were rather different from the other alkali metal atoms and they used different techniques to probe the sample. Attainment of BEC in hydrogen required 22 years of research effort which was a revolution in techniques for cooling and manipulating atoms using laser-based

methods. In this chapter I will briefly summarize the method of cooling process and a technique to study BEC in hydrogen atoms.

3.1 The Basic of Trapping and Cooling Hydrogen

Spin polarized hydrogen is created by the magnetic state selection of hydrogen at a cryogenic temperature. In high magnetic fields the electron and proton spin quantum numbers are $m_e = -\frac{1}{2}$, $m_p = \pm\frac{1}{2}$ for $H \downarrow$ and $m_e = +\frac{1}{2}, m_p = \pm\frac{1}{2}$ for $H \uparrow$ which the spins of the 1S state of atomic hydrogen can couple in four ways. The four hyperfine states are labeled a-d as shown in Figure 3.1. The lowest two states a and b are pulled toward regions of high magnetic field, and the low field seeking states (c and d) are expelled from high field regions.

At the beginning of an experiment [5], molecular hydrogen is loaded into the cryogenic apparatus by blowing a mixture of H_2 and ^4He into a cold can ($T \approx 1$ K). The H_2 molecules are dissociated by pulsing an rf discharge in a region of 4 T magnetic field. The low field seekers are blown into a confinement cell in the trap. The trap field are created by currents in superconducting coils which create a trap with maximum trap depth 0.82 T. The trap depth is the difference between the field at maximum field and the minimum field in the center of the trap. There are seventeen independently controlled coils in the apparatus which are used to adjust the trap shape.

สถาบันวิทยบริการ
จุฬาลงกรณ์มหาวิทยาลัย

The magnetic trap consists of a long quadrupole field to confine the atoms radially with axial solenoids at each end to provide axial confinement an elongated

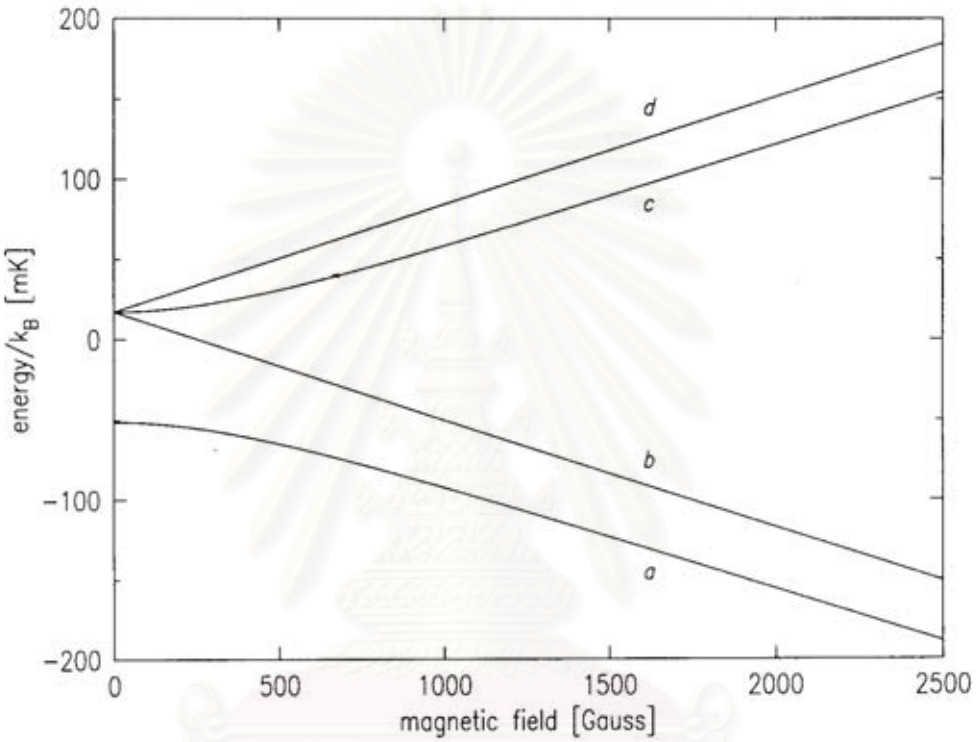

Figure 3.3: Hyperfine diagram for the ground state of atomic hydrogen [2].

สถาบันวิทยบริการ
จุฬาลงกรณ์มหาวิทยาลัย

variant of the Ioffe-Pritchard configuration (labeled "IP"), as shown in Figure 3.2. The field increases linearly away from the z axis of the trap (the potential exhibits near cylindrical symmetry about the z axis); the potential is small and roughly uniform for about 20 cm along the z axis.

The trapping fields are produced inside a cell that confines the gas cloud while atoms are loaded into the trap. For trapped atoms, their total energy must be less than the trap depth. Two techniques are used to cool the atoms into the trap. First, superfluid ^{4}He film is covered the walls and reduces the binding energy of the H atoms. In order to prevent the hot atoms stick tightly to the cold surfaces. The second stage of cooling involves collisions among the atoms that are crossing the trap region. Sometimes these collisions result in one atom having low enough energy to become trapped. The partner atom in the collision goes to the wall and is thermalized.

The cell walls are quickly cooled to below 150 mK. At this temperatures the residence times of the atoms on the surface of the cell are much longer than the recombination time, and so the surface is sticky. The warm atoms go to the surface recombine before having a chance to leave the surface. Thus no warm particles can leave the wall and carry energy to the trapped gas.

Both d and c low field seeking states are caught in the trap. However, inelastic collision processes involving two c state atoms quickly deplete the c state population, and remaining atoms constitute a doubly polarized sample (both electron and proton spins are polarized). For peak densities in the normal gas of $n = 10^{14}\text{cm}^{-3}$ the characteristic decay time is 40 s.

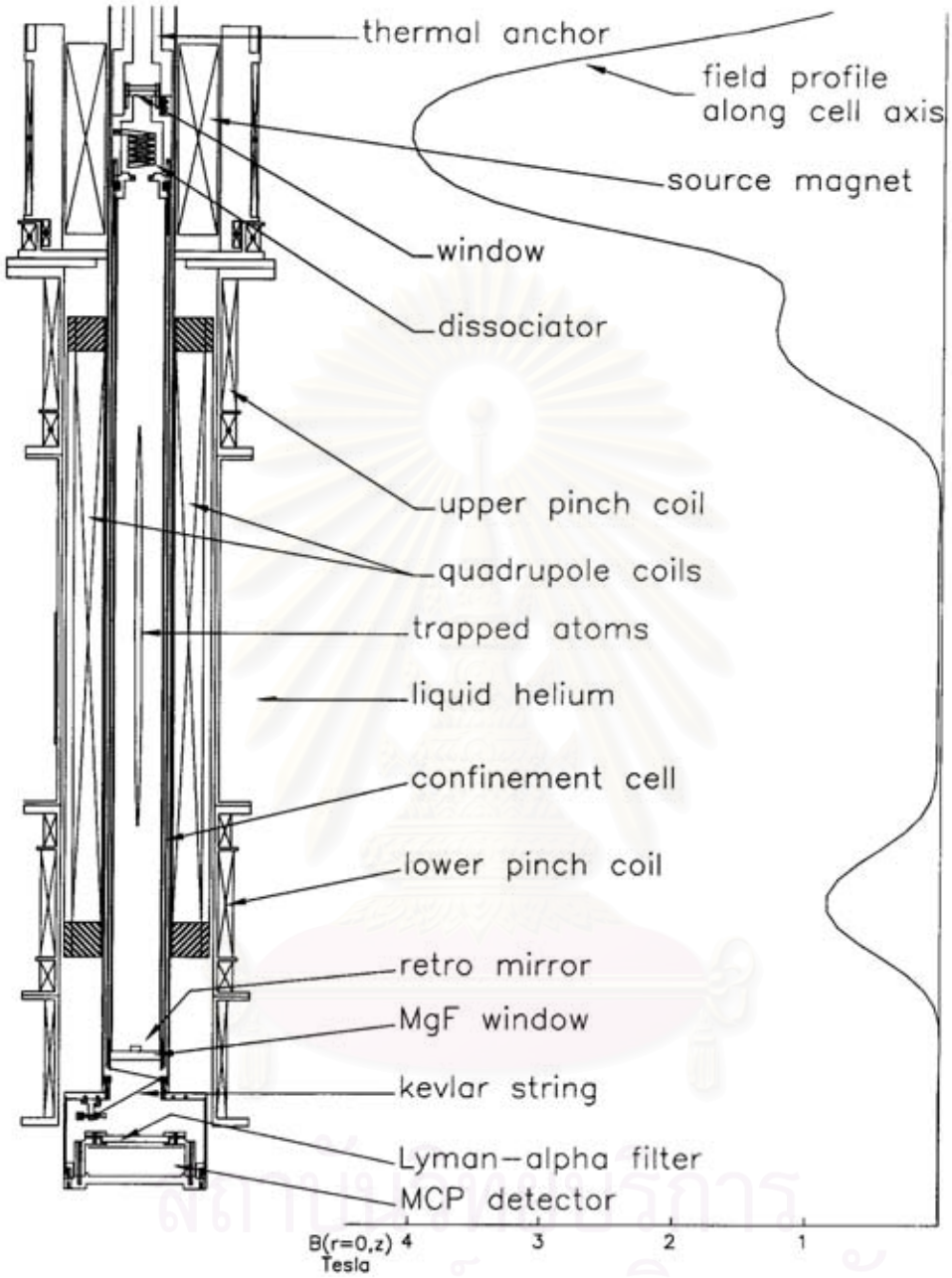

Figure 3.4: Cutaway diagram of the system [2].

3.2 Evaporation Techniques

Evaporative cooling occurs when highly energetic atoms are permitted to escape over a saddle point in the magnetic field at one end of the trap. Evaporation is forced by lowering this axial confinement field while simultaneously holding the radial confinement field fixed. Energetic atoms are able to escape out the end of the trap. With this method, called saddle point evaporation, it was possible to achieve conditions close to BEC in hydrogen but the cooling power is not adequate to cross barrier. Evaporation requires collisions for maintaining thermal equilibrium as the system cools. Because of hydrogen's small scattering length, its collision cross section is small and evaporation is much slower than in other alkali metal atoms.

In saddle point evaporation of harmonic trap, atoms escape only along the z-axis. For atom to escape, it must have a sufficient energy in the axial degree of freedom [11], $E_Z \geq V_{trap}$, where V_{trap} is the trap depth as set by the saddle point potential. Because only the z-motion is involved, the evaporation is one-dimensional. To solve this problem the magnetic trap often called the "Ioffe-Pritchard" type (abbreviated as "IP") was used. This magnetic trap causes mixing energy in axial and radial degree of freedom thus all atoms with total energy $E \geq V_{trap}$ can promptly escape. The energy mixing will be explained theoretically in Chapter 4.

As the energy decreases and the IP trap becomes more harmonic, the mixing time lengthens. When it becomes comparable to the collision time, the evaporation rate falls [11]. To solve this problem the technique of rf evaporation below 120 K, which permits evaporation in three dimensions, was used. A radio-frequency magnetic field drives transitions between the trapped state and some

other (untrapped) hyperfine sub-level, causing the atom to be ejected from the trap. In hydrogen the trapped hyperfine state is $(F = 1, m = 1)$. By starting with an rf field resonant with the highest fields in the trap, then slowly lowering the frequency, successively lower energy atoms can be expelled. Since all the atoms on a specific energy surface in the trap are affected, the process is more efficient than saddle point evaporation. This process allowed us to achieve the conditions necessary for BEC. Figure 3.3. summarizes the entire cooling process.

3.3 Observation of BEC

We now describe the first observations of Bose-Einstein condensation of hydrogen atom. The technique was used in the experiment is laser spectroscopy. By this probe, we are able to monitor the density and temperature of the gas as the temperature is reduced by rf evaporation. When the gas is cooled into the quantum degenerate regime, signatures of the Bose-Einstein condensate appear in the spectrum; these can be analyzed to reveal the size and population of the condensate.

3.3.1 Two-Photon Spectroscopy

Since the energy levels in hydrogen atoms are so widely spaced, two-photon spectroscopy of 1S-2S transition was used to study the trapped hydrogen atoms [12]. When illuminated with photons of energy exactly half the 1S to 2S level spacing, the atoms are promoted to the 2S state by absorbing the two photons (see Figure 3.4). This differs from the one photon process used to manipulate and study the alkali-metals in two important ways [13]. First, the resonance is extremely

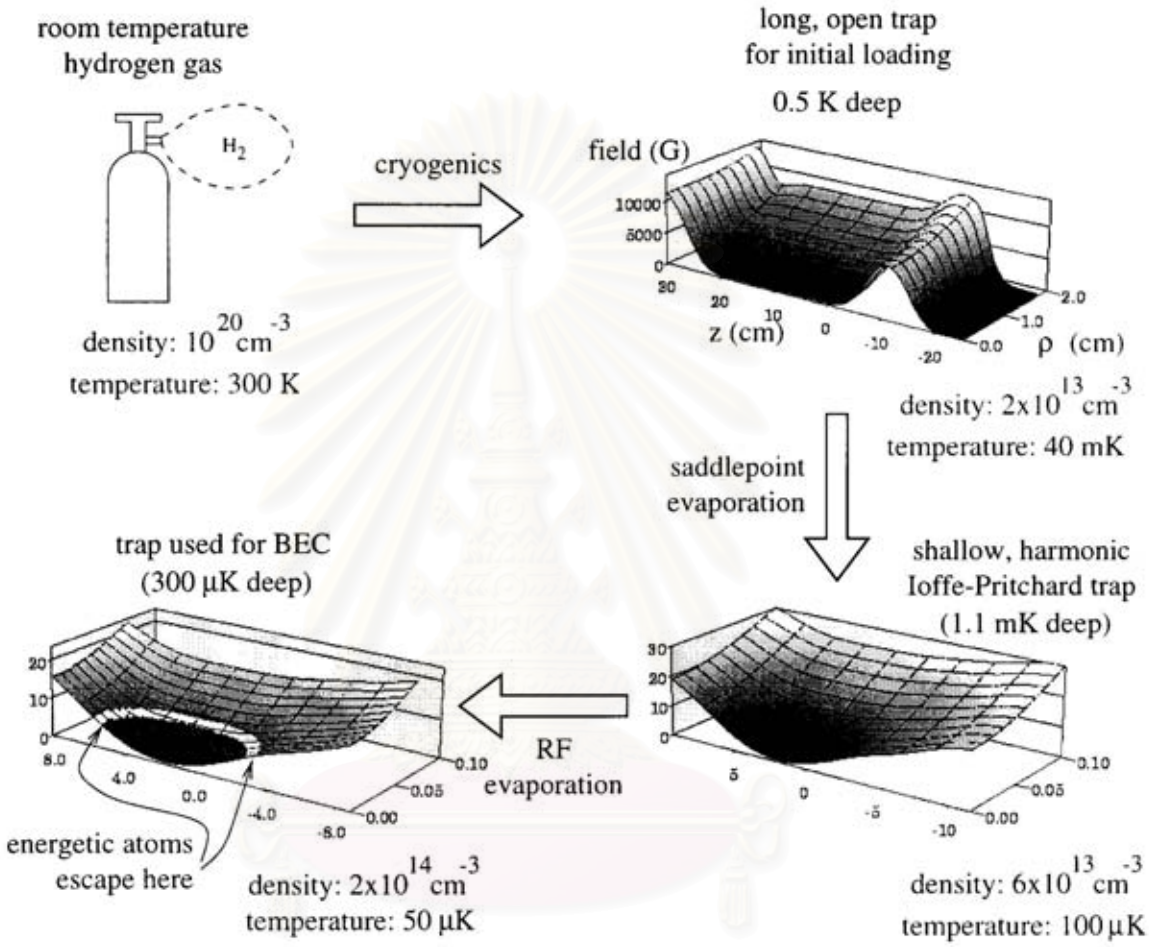

Figure 3.5: Schematic diagram of the cooling process [2].

สถาบันวิทยบริการ
จุฬาลงกรณ์มหาวิทยาลัย

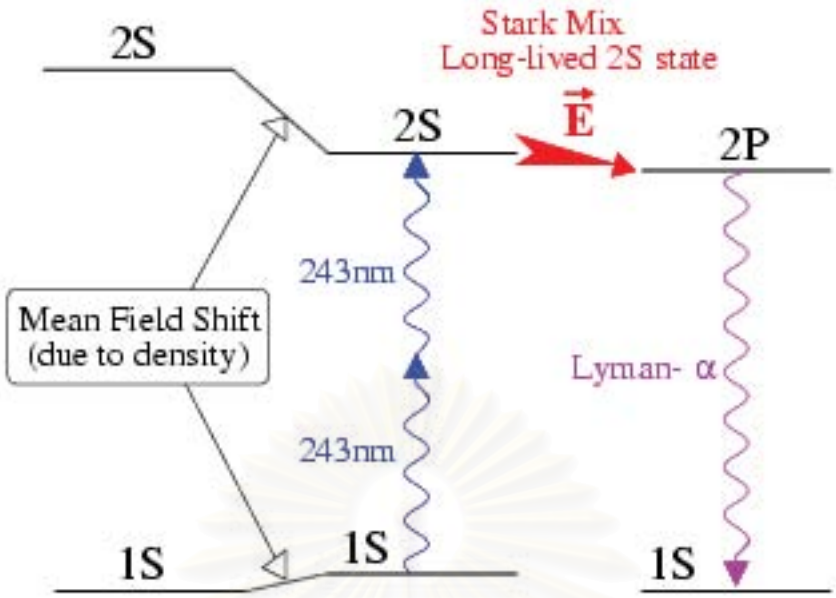

Figure 3.6: Two-photon spectroscopy of the 1S-2S transition in hydrogen [3].

narrow allowing it to be used for very high resolution spectroscopy. Second, the absorption is so weak that the resonance can not be detected by decreasing the amplitude of the transmitted beam. Instead, an electric field is applied to the atoms which mixes the long lived 2S state with the short lived 2P state. The atom then returns to the ground state by emitting of a Lyman-α photon. The resonance is detected by recording the Lyman-α production as a function of the frequency of the illuminating beam.

In the experiment a laser beam of 243 nm is reflected back on itself by a mirror at the bottom of the cell creating a standing wave in the trap. In this configuration the atom may absorb two photons from the same beam or one photon from each beam. Atoms that absorb two co-propagating photons produce a recoil shift and Doppler broadened feature in the spectrum [13] (see Fig. 3.5). The excitation is said to be "Doppler-sensitive." The shape of the Doppler line

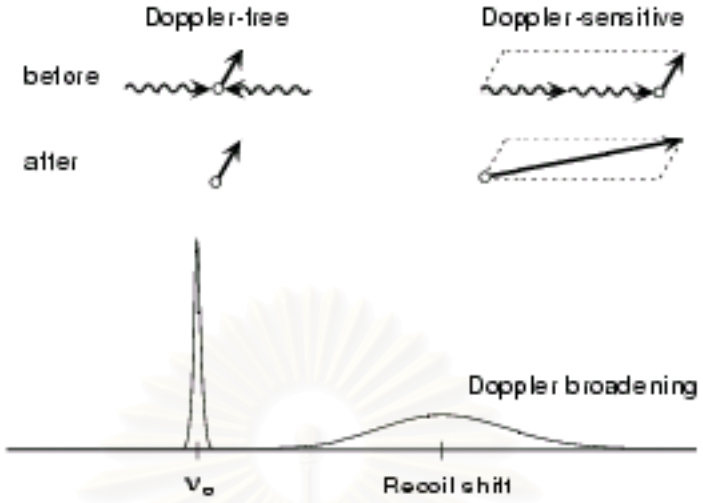

Figure 3.7: Feature of the two-photon spectrum in a standing wave [3].

gives the momentum distribution of the gas and thus provides another measure of the temperature. On the other hand, no momentum is transfered to the atoms that absorb two counter-propagating photons, and the excitation is said to be "Doppler-free." This effect can be used to measure sample density.

The energy equation for two-photon excitation of an isolated atom from state i to state f, with initial momentum $\mathbf{P}_i$ and final momentum $\mathbf{P}_f = \mathbf{P}_i + \hbar(\mathbf{k}_1 + \mathbf{k}_2)$, where $\mathbf{k}_1$ and $\mathbf{k}_2$ are the wave vectors of the laser beams, is [5]

$$2h\nu = \sqrt{P_f^2c^2 + (mc^2 + 2\hbar\nu_0)^2} - \sqrt{P_i^2c^2 + (mc^2)^2} \tag{3.1}$$

where the rest mass of the atom in the initial state is m, ν is the laser frequency and $2\nu_0 = 2.466\times10^{15}Hz$ [14] is the unperturbed transition frequency. Expanding

Eq.(3.1), we obtain ν

$$\nu = \nu_0 + \underbrace{\frac{(\mathbf{k_1}+\mathbf{k_2})\cdot P_i}{4\pi m}(1-\varepsilon)}_{\triangle\nu_{D_1}} + \underbrace{\frac{\hbar(\mathbf{k_1}+\mathbf{k_2})^2}{8\pi m}(1-\varepsilon)}_{\triangle\nu_R} - \underbrace{\frac{\nu_0 P_i^2}{2(mc)^2}}_{\triangle\nu_{D_2}} + O(\varepsilon^3) \qquad (3.2)$$

Here $\triangle\nu_{D1}$and $\triangle\nu_{D2}$ are the first and second order Doppler shifts, respectively, $\triangle\nu_R$ is recoil shift and $\varepsilon = \frac{2h\nu_0}{mc^2} = 1.1 \times 10^{-8}$ [5] is a relativistic correction which accounts for the mass change of the atom upon absorbing energy $2\hbar\nu_0$. For hydrogen in the submillikelvin regime, $\triangle\nu_R << 1$ Hz and can be neglected.

In the Doppler-sensitive configuration, $\mathbf{k_1} = \mathbf{k_2}$ and $\triangle\nu_R = 6.7$ MHz [5]. At temperature of 50 μK, $\triangle\nu_{D_1} \sim 2.6$ MHz, and thus the Doppler-sensitive peak is well separated from the Doppler-free. In the Doppler-free configuration, $\mathbf{k_1} = -\mathbf{k_2}$, and there is no recoil or first order Doppler broadening.

3.3.2 The 1S-2S Spectrum of a Non-Degenerate Gas

The spectrum of the trapped hydrogen gas slightly above the quantum degenerate regime is shown in Figure 3.6. There are two components of the spectrum, corresponding to absorption of co-propagating or counter-propagating photons.

The wide, low feature on the right is the Doppler sensitive which is the Gaussian line shape expected for a Maxwell-Boltzmann distribution of kinetic energies in a sample at 42 μK [5]. The Doppler sensitive spectrum maps the velocity distribution through the Doppler shift. The Doppler free spectrum gives information about the density distribution. At this low temperature the recoil-shifted Doppler-sensitive line is clearly separated from the Doppler-free line.

3.3.3 Cold-Collision Frequency Shift

The density and temperature are measured through the cold collision frequency shift. At low temperatures, in the limit $a \ll \lambda$ (thermal de Broglie wavelength),

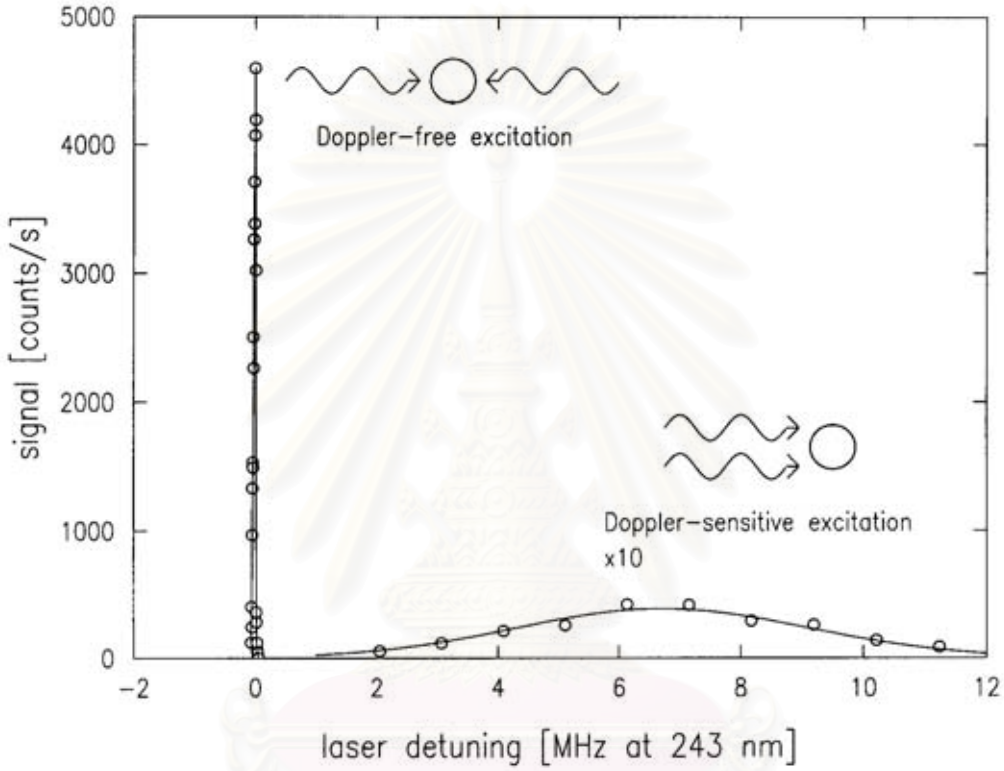

Figure 3.8: The spectrum of non-degenerate gas [2].

สถาบันวิทยบริการ
จุฬาลงกรณ์มหาวิทยาลัย

only S-wave collisions are important. These collisions give rise to a mean field interaction energy, and they introduce frequency shift into radiative transition. In the presence of a could of atoms of density n in the 1S state, an atom in state σ experiences a shift of its energy by an amount

$$\triangle E = \frac{4\pi\hbar^2 a_{\sigma-1S} n}{m} g_2(0), \tag{3.3}$$

where m is the atomic mass and $a_{\sigma-1S}$ is the s-wave scattering length which parameterizes collisions between atoms in state σ and in the 1S state. The density normalized second order correlation function $g_2(x)$ is [15]

$$g_2(x) = \frac{1}{nN} \sum_{i \neq j} \langle \Psi \left| \delta \left(r_i - r_j - x \right) \right| \Psi \rangle \, . \tag{3.4}$$

Here Ψ is the wave function for the system and N is the total number of condensate atoms. (For a Bose gas far from degeneracy, $g_2(0) = 2$) Because the scattering lengths for 1S-1S and 1S-2S collision are not identical, the energy to excite an atom to 2S state from a gas of 1S atoms is shifted by an amount

$$\hbar\triangle\nu_{1S-2S} = \frac{4\pi\hbar^2 n}{m} \left(a_{1S-2S} - a_{1S-1S} \right) g_2(0). \tag{3.5}$$

The frequency shift $\triangle\nu_{1S-2S}$ is known as a cold collision frequency shift. For non-degenerate gas the two-photon sum frequency is by $\triangle\nu_{1S-2S} = n\chi$, where $\chi = 4\pi\hbar g_2(0)(a_{1S-2S} - a_{1S-1S})/m$. Once χ is known, the density can be determined directly by measuring the frequency shift. In addition, a measurement of χ can be used to check the theoretical calculations of the scattering lengths. The 1S-1S scattering length is known accurately from theory: $a_{1S-1S} = 0.0648$ Å and a_{1S-2S} has also been computed: $a_{1S-2S} = -2.3$ nm [8].

To measure the frequency shift parameter χ, a series of line scans were taken at different densities as shown in Figure 3.7. The first scan is at the

maximum density and exhibits the largest red shift. Subsequent scans, at lower densities, are smaller and less shift. The area under each photoexcitation curve is proportional to the total number of atoms. Five of the forty spectra are shown. From a plot of frequency V.S. density (see Figure 3.7b), the value of χ can be determined. From a series of such measurements taken at different densities and temperatures, the value of χ is [16]

$$\chi_m = -3.8 \pm 0.8 \times 10^{-10}\ nHzcm^3, \tag{3.6}$$

where χ_m is the (two photon sum) frequency shift per unit density for excitation out of condensate ($g_2(0) = 2$). The theory of cold-collision frequency shift inhomogeneous system is not yet fully understood [11], with the above value of χ_m, one deduces that $a_{1S-2S} = -1.4$ nm, in fair agreement with the prediction. The process leads to a frequency shift proportional to sample density, and thus the spectroscopy is a valuable tool for measuring the sample density which is measured for densities in the range 2 - 7 $\times$ 10^{-13} cm^{-3} and for temperatures between 100 and 500 μK [5].

3.3.4 Spectroscopic Study of the Degenerate Gas

Bose-Einstein condensation involves the macroscopic occupation of the lowest energy quantum state of the system. In a trap this state is concentrated at the minimum of the trapping potential, and it has very small kinetic energy. When the sample is cooled into the quantum degenerate regime the signature of the condensate in 1S-2S spectrum of the gas can be observed. In the Doppler-sensitive spectrum, which maps the momentum distribution, one would expect an intense line at zero detuning from the recoil shift $\triangle\nu_R$, rising above the background spectrum [17]. Figure 3.8 shows the Doppler-sensitive spectrum of the normal

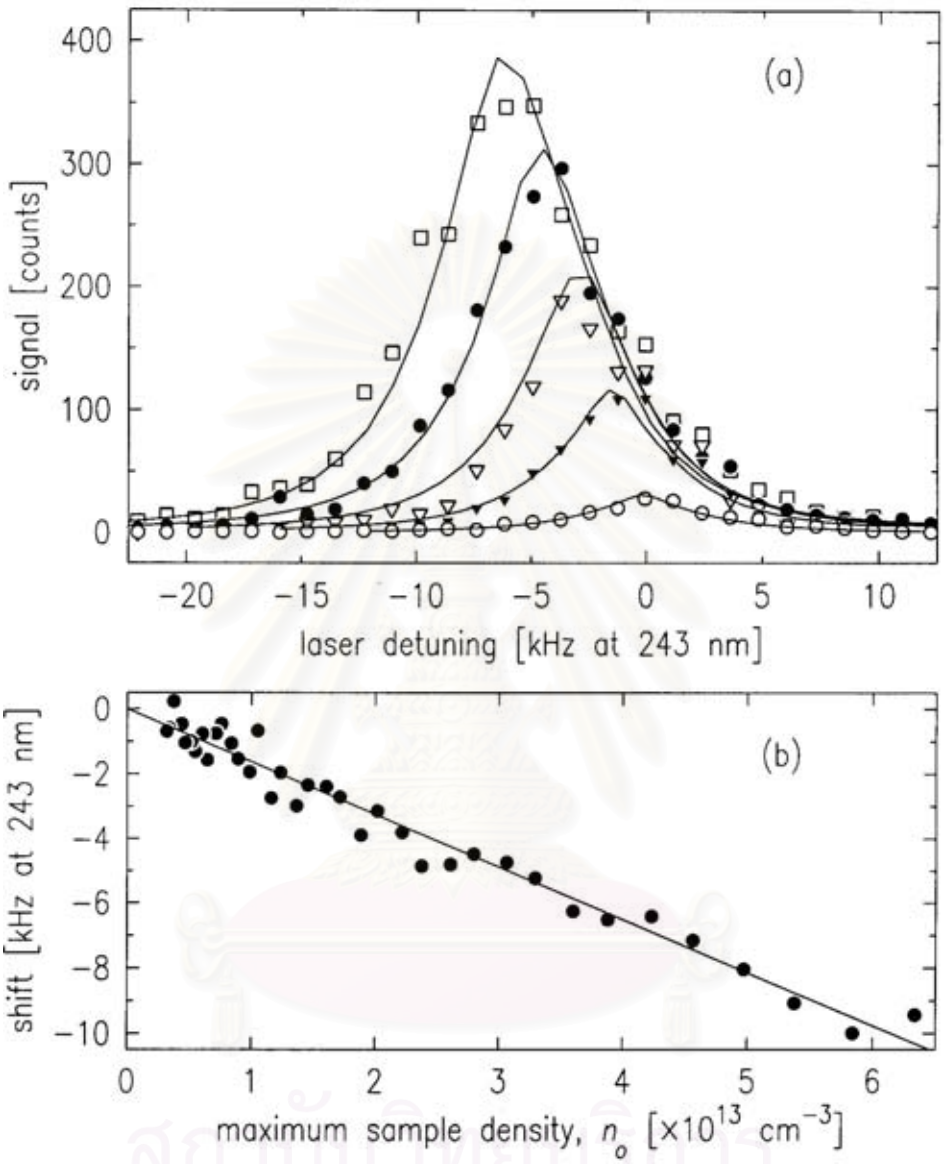

Figure 3.9: Series of spectra of single sample used for a measurement of χ [2].

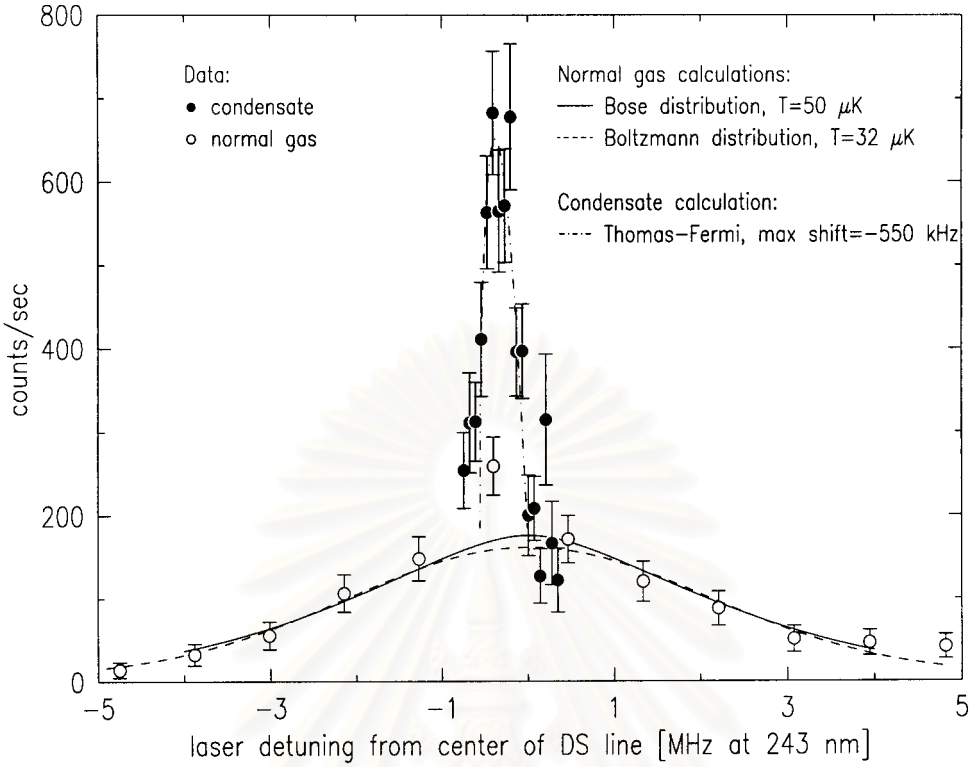

Figure 3.10: Doppler-sensitive spectrum of degenerate gas [2].

gas and the condensate together. Zero detuning is taken at the center of the recoil-shifted spectrum, which is detuned at 6.70 MHz blue of the Doppler-free resonance. Open circles are for normal gas, filled circles are for the condensate gas. The dashed line is a fit to the normal fraction data which assumes a Maxwell-Boltzmann velocity distribution. The dashed line is a calculation which assumes a Bose-Einstein distribution. The dot-dashed line is the condensate spectrum expected for a Thomas-Fermi wave function in a harmonic trap, when the dominate spectral broadening is the cold-collision frequency shift. The temperature of the Bose calculation was chosen to fit the observed spectrum.

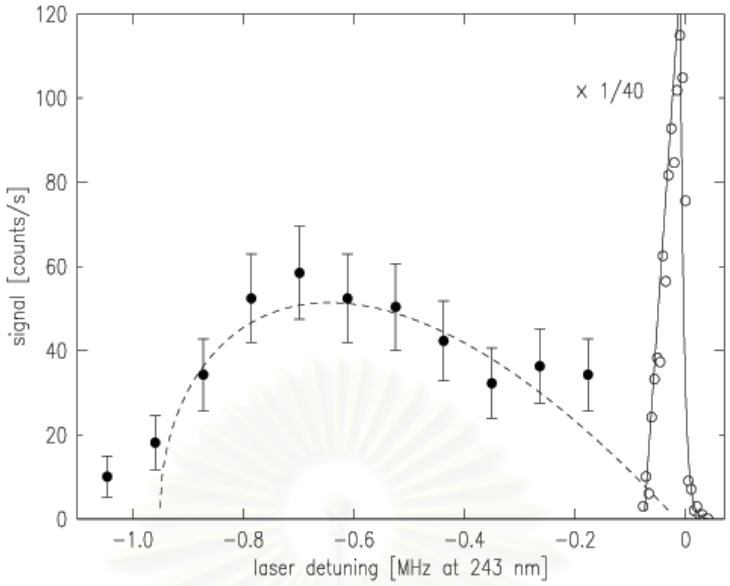

Figure 3.11: Doppler-free spectrum of degenerate gas [2].

3.3.5 Peak Condensate Density

The Doppler-free spectrum is shown in Figure 3.9. It can be used to evaluate the density of the condensate. Atoms excited from different regions of the condensate correspond to different frequency shifts. The signal size at a given detuning $\triangle_p$ is proportional to the number of the condensate atoms on a surface of constant density (see Eq.(3.5)) $n_{cond} = 2\triangle_p/\chi_m$. (assuming $\chi_m = \chi_c$; where χ_c is the frequency shift per unit density for condensate gas)

The intense, narrow feature on the right is due to the normal gas, and is shrunk vertically by a factor 40 to fit in the plot. The wide low, red-shifted feature is the condensate. The line shape is that expected for a Thomas-Fermi wave function in a harmonic trap. The peak shift, $\triangle_p$, is 920 ± 70 kHz, which indicates a peak condensate density $n_p = 2\triangle_p/\chi_m = 4.8 \pm 0.4 \times 10^{15}$ cm^{-3} [5].

3.4 Properties of BEC in Hydrogen

The peak condensate density indicates the number of atoms in the condensate. The population of the condensate is easily computed using the Thomas-Fermi wave-function in the bottom of the Ioffe-Pritchard trap, which is parabolic for condensate size. We approximate the potential energy density of states $\rho(\varepsilon)$ is the differential volume of real space corresponding to a total particle energy. The potential energy density of state function is [5]

$$\rho(\varepsilon) = \int d^3 r \delta(V(r) - \varepsilon). \tag{3.7}$$

The trap shapes in the experiment is called the Ioffe-Pritchard, which has the form [5]

$$V_{IP}(\rho, z) = \sqrt{(\alpha\rho)^2 + (\beta z^2 + \theta)^2} - \theta \tag{3.8}$$

with radial potential energy gradient α, axial potential energy curvature 2β (units of energy/distance^2), and bias potential energy θ. The potential energy density of states for this trap is then

$$\rho(\varepsilon) = \frac{4\pi}{\alpha^2\sqrt{\beta}}\sqrt{\varepsilon}(\varepsilon + \theta). \tag{3.9}$$

We approximate the potential energy density state by $\rho(\varepsilon) = \frac{4\pi}{\alpha^2\sqrt{\beta}}\sqrt{\varepsilon}\theta$ and obtain

$$\begin{aligned} N_c &= \int_0^{\mu} \rho(\varepsilon) n_{cond}(\varepsilon) d\varepsilon \\ &= \frac{16}{15}\frac{\pi\theta}{\alpha^2\sqrt{\beta}} U_0^{3/2} n_p^{5/2}, \end{aligned} \tag{3.10}$$

Where $n_{cond}(\varepsilon) = n_p - \varepsilon/U_0$ is the condensate density (see Eq.(2.6)). From the experiment [5], the peak shift of $\triangle = 620 \pm 20$ kHz corresponds to peak density

$3.26 \pm 0.10 \times 10^{15}$ cm^{-3} and the condensate population is $N_c = 1.19 \pm 0.10 \times 10^9$ atoms. The chemical potential for this peak density is $\mu/k_B = n_p U_0 = 1.9$ K. The extent of the Thomas-Fermi wave function is determined from this equation by setting the density to zero at the edge of the condensate

$$n_{cond} U_0 = \mu - V_{IP}(\rho, z) = 0. \tag{3.11}$$

We obtain

$$\rho_{\max} = \frac{1}{\alpha}\sqrt{\mu^2 + 2\mu\theta} = 7.3\ \mu m \tag{3.12}$$

and

$$z_{\max} = \sqrt{\frac{\mu}{\beta}} = 2.8\ mm. \tag{3.13}$$

The huge aspect ratio, ∼400, gives the condensate a thread-like shape. We can write the chemical potential (μ) that explicitly depends on N_c. For Ioffe-Pritchard trap, it can be shown that

$$n_p = \left(\frac{15\alpha^2\sqrt{\gamma}N_c}{16\pi U_0^{3/2}}\right)^{2/5}. \tag{3.14}$$

The chemical potential is $\mu(n_c) = U_0 n_p$. It satisfies $\mu(n_c) = \partial E_0/\partial n_c$ and is given by

$$E_0 = \frac{5}{7} n_c \mu(n_c) \tag{3.15}$$

where E_0 is the ground state energy. In the experiment, one can evaluate the ground state energy from the peak condensate density in Doppler free spectrum, n_c from Eq. (3.10) and $U_0/k_B = 3.92 \times 10^{-16}$ μK cm^3 parameterizes the mean field energy. The ground energy of each trap and parameters are summarized in Table 3.1.

The parameters α, γ, and θ describe the Ioffe-Pritchard potential; α, γ are calculated and θ is measured. The peak cold-collision frequency shift in the

Parameter	Trap A		Trap B	
$\alpha/k_B\,(mK/cm)$	15.9		9.5	
$\gamma/k_B\left(\mu K/cm^2\right)$	25		25	
$\theta/kB\,(\mu K)$	35±2		34±2	
$\mathrm{T}_c\,(\mu K)$	∼65		∼50	
$\triangle_p\,(kHz)$	920±70		620±20	
	χ_c=χ_c	χ_c=$\chi_m/2$	χ_c=χ_c	χ_c=$\chi_m/2$
$n_p\,(\times 10^{15} cm^{-3})$	4.8±0.4±1	9.7±0.7±2	3.3±0.1±0.7	6.5±0.2±1.3
$N_c\,(\times 10^9)$	1.2±0.2	6.6±1.3	1.2±0.1	6.7±0.5
$\mu/k_B\,(\mu K)$	1.9	3.8	1.3	2.6
$2\rho_{\max}\,(\mu m)$	15	21	20	28
$2z_{\max}\,(mm)$	5.5	7.8	4.5	6.4
$\mathrm{E}_c = \frac{5}{7}N_c\mu$ (J)	2.25×10^{-20}	2.47×10^{-19}	1.54×10^{-20}	1.67×10^{-19}

Table 3.2: Summary of parameter describing the two trap shapes used for achieving BEC and summary of the properties of the condensates [2].

condensate is $\triangle_p$. The remainder of the table is divided to show the implications of assuming $\chi_c = \chi_m$ or $\chi_c = \chi_m/2$. The peak condensate density is n_p, chemical potential is μ and total condensate energy is E_c. The number of condensate atoms is N_c. Finally, the length and diameter of the condensates are given. The uncertainties are divided into a component which depends on the present experiment (first number), and a component reflecting the 20% uncertainty on χ_m (second number).

A thorough treatment of the relation between χ_c and χ_m has been undertaken by Killian [15]. He concludes that $\chi_c = \chi_m/2$ because exchange effects should be present in the normal gas, but absent in a condensate. Here, the experimental evidence suggests that perhaps $\chi_c = \chi_m$. Firstly if we take $\chi_c = \chi_m/2$ then the number of atoms lost, as described in Fried's thesis [5], is as large as the total original population of the trap. Secondly the condensate fraction measured spectroscopically agrees well with the fraction one computes

from the population in the condensate by assuming that $\chi_c = \chi_m$. If $\chi_c = \chi_m/2$ then the calculated condensate fraction is $2^{5/2} \simeq 6$ times larger than indicated by the spectroscopic technique. Therefore the possibility should be explored that $\chi = 2\hbar\left(a_{1S-2S} - a_{1S-1S}\right)/m$ (instead of $\chi = 4\hbar\left(a_{1S-2S} - a_{1S-1S}\right)/m$) for excitation out of the thermal gas. There are significant ambiguities so that this problem clearly requires further study.

สถาบันวิทยบริการ
จุฬาลงกรณ์มหาวิทยาลัย

Chapter 4
Theoretical Considerations

Having discussed the experimental aspect of Bose-Einstein condensation of atomic hydrogen in Chapter 3, we now turn to the theoretical aspect of the phenomena in this chapter. First, we explain why pervious experiments could not bring trapped hydrogen into the quantum degenerate regime and how the Ioffe-Pritchard trap influences the trapped gas. We then apply the techniques from many-body Feynman path integral theory to obtain the ground state properties of the Bose-Einstein condensation of atomic hydrogen confined in the Ioffe-Pritchard trap.

4.1 Ioffe-Pritchard Trap

Previous attempts to obtain BEC in hydrogen failed ([18], [19]) because the cooling process became bottlenecked by the slow rate at which energetic atoms could escape, thus reducing the effective cooling rate. To understand this bottleneck we must first consider the details of the trap shape. We then study the motion of the particles that have enough energy to escape.

The trap shape used to confine samples at $T < 200K$ is often called the Ioffe-Pritchard trap [20]. Using axial coordinate z and radial coordinate ρ, the potential has the from

$$V_{IP}(\rho, z) = \sqrt{(\alpha\rho)^2 + (\gamma z^2 + \theta)^2} - \theta \tag{4.1}$$

with radial potential energy gradient α (J/cm), axial potential energy curvature 2γ (J/cm^2), and bias potential energy θ (J).

In the limit of $\rho << \theta/\alpha$, the Ioffe-Prithchard potential is harmonic in the radial coordinate, as may be seen by expanding the potential in power series

$$V_{IP}(\rho, z) = \gamma z^2 + \frac{1}{2}\frac{\alpha^2}{\gamma z^2 + \theta}\rho^2 + \frac{1}{8}\frac{\alpha^3}{(\gamma z^2 + \theta)^2}\rho^3 + ... \tag{4.2}$$

The trap is harmonic in the radial direction when the third term is much smaller than the second term. The trap appears harmonic in all three directions to short samples for which the radial oscillation frequency is essentially uniform along the length of the sample. This occurs for temperatures $T << 4\theta/k_B$. In the harmonic regime, the axial oscillation frequency is

$$\omega_z = \sqrt{\frac{2\gamma}{m}} \tag{4.3}$$

and the radial oscillation frequency is

$$\omega_\rho = \frac{\alpha}{\sqrt{m(\gamma z^2 + \theta)}}. \tag{4.4}$$

Previous attempts to cool hydrogen to BEC utilized saddlepoint evaporation, in which energetic atoms escape over a saddlepoint in the magnetic field barrier at one end of the trap. To escape, the atom must have energy in axial degree of freedom (z) greater than trap depth. This atom removal technique is inherently one dimensional. The collisions which drive evaporation produce many atoms with high energy in the other degrees of freedom, and in order for these to escape the energy must be transferred to the axial degree of freedom. This energy transfer process was analyzed theoretically by Surkov, Walraven, and Shlyapnikov [21], we now follow their analysis.

In a harmonic trap the potential is separable, and the particle motion is completely regular; no energy exchange occurs. In the Ioffe-Pritchard trap, energy exchange can occur because the potential is not separable; the radial oscillation frequency depends on the axial coordinate, z, and so radial motion can couple to axial motion. (see Eq. (4.4)) Therefore, the evaporation efficiency depends on how strongly the atom's motional degrees of freedom are coupled in the trap. For high trapping field ($T > 1$ mK), the degrees of freedom in Ioffe-Prithchard trap are well coupled, and atomic trajectories are stochastic.

This energy mixing can be understood by considering how rapidly the radial oscillation frequency changes as an atom moves along the z axis. If the frequency changes slowly (adiabatically), then the energy will not mix among the degrees of freedom. The adiabaticity parameter is the fractional change of the radial oscillation frequency in one oscillation period as the atom moves axially through the trap. Strong mixing occurs when [5]

$$\frac{\dot{\omega_\rho}}{\omega_\rho^2} \sim 1. \tag{4.5}$$

Here $\dot{\omega_\rho} = (d\omega_\rho/dz)(dz/dt)$. For a Ioffe-Prithchard trap with a bias that is large compared to $k_B T$, $\omega_\rho = \alpha/\sqrt{(\gamma z^2 + \theta)m}$. We have used the expansion in Eq. (4.2), which is valid if $k_B T \sim \alpha\rho << \theta$. Given that $k_B T << \theta$, the adiabaticity parameter is

$$\frac{\dot{\omega_\rho}}{\omega_\rho^2} = v_z \frac{\gamma z\sqrt{m}}{\alpha\sqrt{\gamma z^2 + \theta}}. \tag{4.6}$$

We see that several factors contribute to good mixing: large axial velocity v_z (which occurs at high temperatures), small radial gradient α, small bias field θ, and large axial curvature γ. In practice, however, achieving BEC requires low temperatures (v_z small) and high densities (obtained with large compressions, and

thus large α). Consequently, the degrees of freedom do not mix and evaporation becomes essentially one dimensional. Typical values for the experiment [5] are $\alpha/k_B = 16$ mK/cm, $\gamma/k_B = 25$ K/cm^2, $\theta/k_B = 30$ K, $T = 100$ K, $z \sim 2$ cm, and $v_z = 140$ cm/s, so that $\dot{\omega_\rho}\ /\omega_\rho^2 \sim 10^{-3}$. For these conditions it takes about 10^3 oscillations to transfer energy. There is not enough time to transfer the radial energy to axial energy before the particle has a collision. The energy mixing is thus very weak and the evaporation is one dimensional. The evaporative cooling power thus drops dramatically. Experiments have confirmed that phase space compression ceases near 100 μK.

In order to maintain the evaporation efficiency a technique is required that quickly removes all particles with energy greater than the trap depth. To this end they implemented rf evaporation as described in details in Chapter 3.

4.2 Many-Body Feynman Path Integral Theory

In this section we calculate the ground state properties of atomic hydrogen using Feynman's path integral theory with the assistance of the variational principle. First we consider N hydrogen atoms in Ioffe-Pritchard trap. Retaining only the first two terms in the expansion (4.2) and treating the interaction among hydrogen atoms as mean-field energy, which are repulsive for s-wave scattering lengths $a > 0$. The Lagrangian for the entire system is

$$L = \frac{m}{2}\sum_{i=1}^{N}(\dot{x}_i^2 + \dot{y}_i^2 + \dot{z}_i^2) - \sum_{i=1}^{N}[\gamma z_i^2 + \frac{\alpha^2}{2(\gamma z_i^2 + \theta)}(x_i^2 + y_i^2)] - (\frac{4\pi\hbar^2 a}{m})\sum_{ij}^{N}\delta(r_i - r_j) \tag{4.7}$$

We use the trial action, which can be solved the density matrix exactly and Lagrangian of the trial action must be similar to Lagrangian of the real

system. So we choose

$$S_0 = \int_0^T \left(\frac{m}{2} \sum_{i=1}^{N} (\dot{x}_i^2 + \dot{y}_i^2 + \dot{z}_i^2) - \sum_{i=1}^{N} [\omega_z z_i^2 + \omega_\rho (x_i^2 + y_i^2)] \right) dt. \tag{4.8}$$

We now find the density matrix of the system. The formulation of the density matrix bears a close resemblance to the general expression for the kernel, which was derived in Chapter 4 of the Feynman and Hibb's book [22]. If the time of the kernel is replaced by $-i\beta\hbar$, the expression for the density matrix is identical to the expression for the kernel corresponding to an imaginary time interval. We thus find the kernel first. It has the form

$$K = \int_{r1}^{r_2} e^{\frac{i}{\hbar}S} Dr(t) = \int_{r_1}^{r_2} e^{\frac{i}{\hbar}S_0} Dr(t) \cdot \frac{\int_{r1}^{r_2} e^{\frac{i}{\hbar}(S-S_0)} e^{\frac{i}{\hbar}S_0} Dr(t)}{\int_{r1}^{r_2} e^{\frac{i}{\hbar}S_0} Dr(t)}. \tag{4.9}$$

The second factor of Eq. (4.9) has the form of an average of $e^{\frac{i}{\hbar}(S-S_0)}$ with $e^{\frac{i}{\hbar}S_0}$ as the weighting factor for each path $r(t)$. We thus write Eq. (4.9) as

$$K = K_0 \cdot \left\langle e^{\frac{i}{\hbar}(S-S_0)} \right\rangle_{S_0} \tag{4.10}$$

where

$$K_0 = \int_{r_2}^{r_1} e^{\frac{i}{\hbar}S_0} Dr(t). \tag{4.11}$$

Since $\frac{i}{\hbar}S$ and $\frac{i}{\hbar}S_0$ are real if time is imaginary, then we can use the inequality [9]

$$\left\langle e^{-x} \right\rangle \geq e^{-\langle x \rangle}. \tag{4.12}$$

The geometrical interpretation of this relation is shown in Fig.(4.1). Note that Eq. (4.12) does not depend on how the $\langle x \rangle$ are distributed. Applying Eq. (4.12) to Eq. (4.10), we can find

$$K \geq K_0 e^{\left\langle \frac{i}{\hbar}(S-S_0) \right\rangle_{S_0}}. \tag{4.13}$$

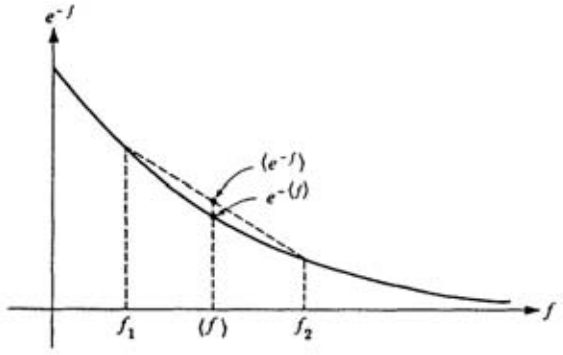

Figure 4.12: Geometrical interpretation of $\left\langle e^{-f}\right\rangle \geq e^{\langle -f\rangle}$ [1].

This relation is true when we replace the time by $-i\beta\hbar$. The exponent in Eq. (4.13) has the explicit from

$$\langle S - S_0\rangle = \int_0^T dt\, \langle L - L_0\rangle_{S_0} \tag{4.14}$$

or

$$\begin{aligned}\langle S - S_0\rangle \;=\; & \int_0^T dt \sum_{i=1}^{N}(\frac{m}{2}\omega_z^2 - \gamma)\left\langle z^2\right\rangle_{S_0} + \int_0^T dt \sum_{i=1}^{N}\frac{m}{2}\omega_\rho^2(\left\langle x^2\right\rangle_{S_0} + \left\langle y^2\right\rangle_{S_0}) \\ & - \int_0^T dt \sum_{i=1}^{N}\frac{\alpha^2}{2}\left\langle \frac{(x^2+y^2)}{\gamma z^2+\theta}\right\rangle_{S_0} - \frac{4\pi\hbar^2 a}{m}\sum_{ij}^{N}\int_0^T dt\, \langle\delta(r_i - r_j)\rangle_{S_0}\end{aligned} \tag{4.15}$$

Thus Eq.(4.13) has the explicit form

$$K \geq K_0 \exp\left[\begin{array}{c} \frac{i}{\hbar}\int_0^T dt \left(\begin{array}{c} \sum_{i=1}^{N}(\frac{m}{2}\omega_z^2 - \gamma)\langle z^2\rangle_{S_0} + \sum_{i=1}^{N}\frac{m}{2}\omega_\rho^2(\langle x^2\rangle_{S_0} + \langle y^2\rangle_{S_0}) \\ -\sum_{i=1}^{N}\frac{\alpha^2}{2}\omega_\rho^2\left\langle\frac{(x^2+y^2)}{\gamma z^2+\theta}\right\rangle_{S_0} \end{array}\right) \\ -\frac{i}{\hbar}\left(\frac{4\pi\hbar^2 a}{m}\right)\sum_{ij}^{N}\int_0^T dt\,\langle\delta(r_i - r_j)\rangle_{S_0} \end{array}\right]. \tag{4.16}$$

Replace t by $-i\hbar t$, we obtain the inequality for density matrix

$$\rho \geq \rho_0 \exp\left[\int_0^\beta dt \left(\begin{array}{c} \sum_{i=1}^N (\frac{m}{2}\omega_z^2 - \gamma) \left\langle z^2 \right\rangle_{S_0} + \sum_{i=1}^N \frac{m}{2}\omega_\rho^2 (\left\langle x^2 \right\rangle_{S_0} + \left\langle y^2 \right\rangle_{S_0}) \\ - \sum_{i=1}^N \frac{\alpha^2}{2} \left\langle \frac{(x^2+y^2)}{\gamma z^2+\theta} \right\rangle_{S_0} \\ \left(-\frac{4\pi\hbar^2 a}{m}\right) \sum_{ij}^N \int_0^\beta dt \left\langle \delta(r_i - r_j) \right\rangle_{S_0} \end{array} \right) \right]. \tag{4.17}$$

The parameter t in Eq. (4.17) is not the true time in the usual sense. It is just a parameter in an expression for density matrix ρ. However, if we wish to make use of analogy in our thinking, we can consider t as the time for a certain path.

To evaluate the exponent in Eq. (4.17), we proceed as follow. We first evaluate $\left\langle x^2 \right\rangle_{S_0} \left\langle y^2 \right\rangle_{S_0}$**a**nd $\left\langle z^2 \right\rangle_{S_0}$ To do so, consider the quantity

$$\left\langle e^{[\frac{i}{\hbar}\int f(t)x(t)dt]} \right\rangle = \int_a^b \exp[\frac{i}{\hbar}\left(S - \int f(t)x(t)dt\right)]Dx(t). \tag{4.18}$$

where $f(t)$ is any arbitrary function of time. If the original action S is Gaussian, then the action is

$$S' = S - \int f(t)x(t)dt \tag{4.19}$$

is also Gaussian. Thus the path integral on the right of Eq. (4.18) can be carried out by the methods of section 2.3 in Chapter 2. If S'_{Cl} is the extremum of the action S', then the factor $\exp\left(iS'_{Cl}/\hbar\right)$ can be extracted as a factor of a path integral of Eq. (4.18). The remaining factor is a path integral over the closed paths $y(t)$. The details are shown in section 7.4 Feynman and Hibb's book [22]. The final result is that the path integral on the right of Eq. (4.18) can be reduced to an exponential function multiplied by the transition element $\langle 1 \rangle$.

$$\left\langle e^{[\frac{i}{\hbar}\int f(t)x(t)dt]} \right\rangle = \left\{ \exp[\frac{i}{\hbar}(S'_{Cl} - S_{Cl})] \right\} \langle 1 \rangle . \tag{4.20}$$

The extremum S_{Cl} can be obtained from Eq. (4.20) by setting $f(t)$ to zero and the action of the forced harmonic oscillator is a special case of action $S_{Cl}^{'}$.

From the transition element given by Eq.(4.20) we can obtain the transition element of $x(t)$ by differentiating Eq.(4.20) with respect to $f(t)$,

$$\left\langle x(t)\exp\left[\frac{i}{\hbar}\int f(t)x(t)dt\right]\right\rangle = \frac{\delta S_{Cl}^{'}}{\delta f(t)}\left\{\exp\left[\frac{i}{\hbar}(S_{Cl}^{'}-S_{Cl})\right]\right\}\langle 1\rangle\,. \tag{4.21}$$

Setting $f(t)=0$, we obtain

$$\langle x(t)\rangle = \langle 1\rangle\left[\frac{\delta S_{Cl}^{'}}{\delta f(t)}\right]_{f(t)=0}. \tag{4.22}$$

Similarly, we obtain

$$\left\langle x^2(t)\right\rangle = \langle 1\rangle\left[-\frac{i}{\hbar}\frac{\delta^2 S_{Cl}^{'}}{\delta f(t)^2}+\left(\frac{\delta S_{Cl}^{'}}{\delta f(t)}\right)^2\right]_{f(t)=0}. \tag{4.23}$$

We now use the action $S_{Cl}^{'}$ for the harmonic oscillator driven by an external force $f(t)$,

$$S_{Cl}^{'} = \frac{m\omega}{2\sin\omega T}\left[\begin{array}{c}\cos\omega T(x_2^2+x_1^2)-2x_1x_2+\frac{2x_2}{m\omega}\int\limits_0^T f(t)\sin\omega t dt\\ +\frac{2x_1}{m\omega}\int\limits_0^T f(t)\sin\omega(T-t)dt\\ -\frac{1}{m^2\omega^2}\int\limits_0^T\int\limits_0^T f(t)f(s)\sin\omega(T-t)\sin\omega s ds dt\end{array}\right]. \tag{4.24}$$

Substitute Eq. (4.24) into Eq. (4.23), we obtain

$$\left\langle x^2(t)\right\rangle_{S_0} = \frac{i\hbar}{m\omega}\frac{\sin\omega(T-t)\sin\omega t}{\sin\omega T}+(\frac{x_2\sin\omega t+x_1\sin\omega(T-t)}{\sin\omega T})^2. \tag{4.25}$$

To apply the above result to our case, we replace t by -$i\hbar t$. Using the relation $\sin(-i\omega\hbar t) = -i\sinh\omega\hbar t$, we obtain

$$\left\langle x^2(t)\right\rangle_{S_0} = \frac{\hbar}{m\omega_\rho}\frac{\sinh\omega_\rho\hbar(\beta-t)\sinh\omega_\rho\hbar t}{\sinh\omega_\rho\hbar\beta}+(\frac{x_2\sinh\omega_\rho\hbar t+x_1\sinh\omega_\rho\hbar(\beta-t)}{\sinh\omega_\rho\hbar\beta})^2$$

$$\begin{aligned}\left\langle y^2(t)\right\rangle_{S_0} &= \frac{\hbar}{m\omega_\rho}\frac{\sinh\omega_\rho\hbar(\beta-t)\sinh\omega_\rho\hbar t}{\sinh\omega_\rho\hbar\beta}+(\frac{y_2\sinh\omega_\rho\hbar t+y_1\sinh\omega_\rho\hbar(\beta-t)}{\sinh\omega_\rho\hbar\beta})^2\\ \left\langle z^2(t)\right\rangle_{S_0} &= \frac{\hbar}{m\omega_z}\frac{\sinh\omega_z\hbar(\beta-t)\sinh\omega_z\hbar t}{\sinh\omega_z\hbar\beta}+(\frac{z_2\sinh\omega_z\hbar t+x_1\sinh\omega_z\hbar(\beta-t)}{\sinh\omega_z\hbar\beta})^2\end{aligned} \tag{4.26}$$

We next calculate $\int_o^\beta \langle x^2(t)\rangle_{S_0}\,dt$, $\int_o^\beta \langle y^2(t)\rangle_{S_0}\,dt$ and $\int_o^\beta \langle z^2(t)\rangle_{S_0}\,dt$

$$\begin{aligned}\int_o^\beta \left\langle x^2(t)\right\rangle_{S_0} dt &= \int_o^\beta \frac{\hbar}{m\omega_\rho}\frac{\sinh\omega_\rho\hbar(\beta-t)\sinh\omega_\rho\hbar t}{\sinh\omega_\rho\hbar\beta}dt\\ &\quad+\int_o^\beta(\frac{x_2\sinh\omega_\rho\hbar t+x_1\sinh\omega_\rho\hbar(\beta-t)}{\sinh\omega_\rho\hbar\beta})^2dt.\end{aligned} \tag{4.27}$$

The first term of Eq. (4.27) can be evaluated easily,

$$\int_o^\beta \frac{\hbar}{m\omega_\rho}\frac{\sinh\omega_\rho\hbar(\beta-t)\sinh\omega_\rho\hbar t}{\sinh\omega_\rho\hbar\beta}dt=\frac{\hbar\beta}{2\omega_\rho m}\coth\omega_\rho\hbar\beta-\frac{1}{2\omega_\rho^2 m}. \tag{4.28}$$

Integrating of the second term, we obtain

$$\begin{aligned}&\int_o^\beta(\frac{x_2\sinh\omega_\rho\hbar t+x_1\sinh\omega_\rho\hbar(\beta-t)}{\sinh\omega_\rho\hbar\beta})^2dt\\ =\;& -\frac{x_1x_2}{2\omega_\rho\hbar}csch\omega_\rho\hbar\beta-\frac{x_1x_2}{\omega_\rho\hbar}\coth\omega_\rho\hbar\beta\cosh\omega_\rho\hbar\beta+\frac{x_1x_2}{2\omega_\rho\hbar}\cosh\omega_\rho\hbar\beta csch\omega_\rho\hbar\beta\\ &+x_1x_2\beta\coth\omega_\rho\hbar\beta csch\omega_\rho\hbar\beta+\frac{x_1^2}{2\omega_\rho\hbar}\coth\omega_\rho\hbar\beta-\frac{x_1^2}{2\omega_\rho\hbar}\cosh2\omega_\rho\hbar\coth\omega_\rho\hbar\beta\\ &-\frac{1}{2}(x_1^2+x_2^2)\beta csch\omega_\rho\hbar\beta+\frac{x_2^2}{4\omega_\rho\hbar}(csch\omega_\rho\hbar\beta)^2\sinh2\omega_\rho\hbar\beta\\ &+\frac{x_1^2}{2\omega_\rho\hbar}\cosh2\omega_\rho\hbar\beta\coth\omega_\rho\hbar\beta\end{aligned} \tag{4.29}$$

Using the expansions

$$\mathrm{csch}\omega_\rho\hbar\beta = \frac{2}{e^{\omega_\rho\hbar\beta}(1-e^{-2\omega_\rho\hbar\beta})}=2e^{-\omega_\rho\hbar\beta}(1+e^{-2\omega_\rho\hbar\beta}+e^{-4\omega_\rho\hbar\beta}+...)$$

$$\begin{aligned}
\text{sech}\omega_\rho\hbar\beta &= \frac{2}{e^{\omega_\rho\hbar\beta}(1+e^{-2\omega_\rho\hbar\beta})} = 2e^{-\omega_\rho\hbar\beta}(1-e^{-2\omega_\rho\hbar\beta}+e^{-4\omega_\rho\hbar\beta}+...) \\
\coth\omega_\rho\hbar\beta &= \frac{(e^{-\omega_\rho\hbar\beta}+e^{-\omega_\rho\hbar\beta})}{(e^{-\omega_\rho\hbar\beta}-e^{-\omega_\rho\hbar\beta})} = 1+e^{-2\omega_\rho\hbar\beta}+e^{-4\omega_\rho\hbar\beta}+... \qquad (4.30)
\end{aligned}$$

The coefficient of the lowest order term, we get in Eq. (4.29) and picking

$$\begin{aligned}
\int_o^\beta \left\langle x^2(t)\right\rangle_{S_0} dt &= \left(\frac{\hbar\beta}{2\omega_\rho m}-\frac{1}{2\omega_\rho^2 m}+\frac{\hbar\beta}{2\omega_\rho m}e^{-2\omega_\rho\hbar\beta}+...\right) \\
&\quad +\frac{(x_1^2+x_2^2)}{2\omega_\rho\hbar}-\frac{x_1x_2}{\omega_\rho\hbar}e^{-\omega_\rho\hbar\beta} \\
&\quad +\frac{(x_1+x_2)^2}{\omega_\rho\hbar}e^{-2\omega_\rho\hbar\beta}-\frac{x_1x_2}{\omega_\rho\hbar}e^{-3\omega_\rho\hbar\beta}+... \qquad (4.31)
\end{aligned}$$

Similarly by changing $\langle y^2(t)\rangle_{S_0}$ and $\langle z^2(t)\rangle_{S_0}$ can be obtained the variable x to y and z, respectively.

Our next step is to evaluate decouple, we find $\int_o^\beta \left\langle \frac{x(t)^2}{\gamma z^2+\theta}\right\rangle_{S_0} dt$ and $\int_o^\beta \left\langle \frac{y(t)^2}{\gamma z^2+\theta}\right\rangle_{S_0} dt$. Since all coordinate in S_0

$$\begin{aligned}
\left\langle \frac{x^2(t)}{\gamma z^2+\theta}\right\rangle_{S_0} &= \frac{\int Dx(t)e^{-S_0(x)/\hbar}x^2(t)}{\int Dx(t)e^{-S_0(x)/\hbar}}\frac{\int Dy(t)e^{-S_0(y)/\hbar}}{\int Dy(t)e^{-S_0(y)/\hbar}}\frac{\int Dz(t)e^{-S_0(z)/\hbar}(\frac{1}{\gamma z^2+\theta})}{\int Dz(t)e^{-S_0(z)/\hbar}} \\
&= \left\langle x^2(t)\right\rangle_{S_o(x)}\left\langle \frac{1}{\gamma z^2+\theta}\right\rangle_{S_o(z)} \qquad (4.32)
\end{aligned}$$

Using the identity $\frac{1}{x}=\int_0^\infty e^{-xq}dq$, we may write

$$\frac{1}{\gamma z^2+\theta} = \int_0^\infty e^{-(\gamma z^2+\theta)q}dq. \qquad (4.33)$$

Using the Jenssen inequality from Eq. (4.12), we find

$$\left\langle \frac{1}{\gamma z^2+\theta}\right\rangle_{S_0} \geq \int_0^\infty e^{-(\gamma\left\langle z^2\right\rangle_{S_0}+\theta)q}dq = \frac{1}{\gamma\left\langle z^2\right\rangle_{S_0}+\theta}. \qquad (4.34)$$

Therefore

$$\left\langle \frac{x^2}{\gamma z^2+\theta}\right\rangle_{S_0} \geq \frac{\langle x^2\rangle_{S_0}}{\gamma\left\langle z^2\right\rangle_{S_0}+\theta}. \qquad (4.35)$$

Substituting the results for $\langle x^2\rangle_{S_0}$ and $\langle z^2\rangle_{S_0}$ from Eq. (4.26) into Eq. (4.35) and using the relation

$$\sinh\omega_\rho\hbar(\beta-t)\sinh\omega_\rho\hbar t=\frac{1}{2}\left(\cosh\omega_\rho\hbar\beta-\cosh(2\omega_\rho\hbar t-\omega_\rho\hbar\beta)\right) \tag{4.36}$$

We obtain

$$\begin{aligned}
&\frac{\langle x^2\rangle_{S_0}}{\gamma\langle z^2\rangle_{S_0}+\theta}\\
=\;&\frac{\frac{\hbar}{2m\omega_\rho}\coth\omega_\rho\hbar\beta-\frac{\hbar}{2m\omega_\rho}\frac{\cosh(2\omega_\rho\hbar t-\omega_\rho\hbar\beta)}{\sinh\omega_\rho\hbar\beta}+(\frac{x_2\sinh\omega_\rho\hbar t+x_1\sinh\omega_\rho\hbar(\beta-t)}{\sinh\omega_\rho\hbar\beta})^2}{\frac{\gamma\hbar}{2m\omega_z}\coth\omega_z\hbar\beta-\frac{\gamma\hbar}{2m\omega_z}\frac{\cosh(2\omega_z\hbar t-\omega_z\hbar\beta)}{\sinh\omega_z\hbar\beta}+\gamma(\frac{z_2\sinh\omega_z\hbar t+x_1\sinh\omega_z\hbar(\beta-t)}{\sinh\omega_z\hbar\beta})^2+\theta}\\
=\;&\frac{\omega_z\hbar\coth\omega_\rho\hbar\beta}{\omega_\rho\left(\gamma\hbar\coth\omega_z\hbar\beta+2m\omega_z\theta\right)}\times\\
&\frac{\left(1-\frac{\cosh(2\omega_\rho\hbar t-\omega_\rho\hbar\beta)}{\cosh\omega_\rho\hbar\beta}+\frac{2m\omega_\rho}{\hbar\coth\omega_\rho\hbar\beta}(\frac{x_2\sinh\omega_\rho\hbar t+x_1\sinh\omega_\rho\hbar(\beta-t)}{\sinh\omega_\rho\hbar\beta})^2\right)}{\left(1-\left(\frac{\gamma\hbar\cosh(2\omega_z\hbar t-\omega_z\hbar\beta)}{(\gamma\hbar\coth\omega_z\hbar\beta+2mb\theta)\sinh\omega_z\hbar\beta}-\frac{2m\omega_z\gamma}{(\gamma\hbar\coth\omega_z\hbar\beta+2mb\theta)}(\frac{z_2\sinh\omega_z\hbar t+x_1\sinh\omega_z\hbar(\beta-t)}{\sinh\omega_z\hbar\beta})^2\right)\right)}
\end{aligned} \tag{4.37}$$

We then Expand Eq.(4.37) by using the relation $\frac{1}{1-x}=1+\sum_{n=1}^{\infty}x^n$ and letting

$$\begin{aligned}
f(z_1,z_2)\;=\;&(\frac{\gamma\hbar\cosh(2\omega_z\hbar t-\omega_z\hbar\beta)}{(\gamma\hbar\coth\omega_z\hbar\beta+2m\omega_z\theta)\sinh\omega_z\hbar\beta}-\\
&\frac{2m\omega_z\gamma}{(\gamma\hbar\coth\omega_z\hbar\beta+2m\omega_z\theta)}(\frac{z_2\sinh\omega_z\hbar t+x_1\sinh\omega_z\hbar(\beta-t)}{\sinh\omega_z\hbar\beta})^2),
\end{aligned}$$

We obtain

$$\begin{aligned}
\frac{\langle x^2\rangle_{S_0}}{\gamma\langle z^2\rangle_{S_0}+\theta}\;=\;&\frac{\omega_z\hbar\coth\omega_\rho\hbar\beta}{\omega_\rho\left(\gamma\hbar\coth\omega_z\hbar\beta+2m\omega_z\theta\right)}[1-\frac{\cosh(2\omega_\rho\hbar t-\omega_\rho\hbar\beta)}{\cosh\omega_\rho\hbar\beta}\\
&+\frac{2m\omega_\rho}{\hbar\coth\omega_\rho\hbar\beta}(\frac{x_2\sinh\omega_\rho\hbar t+x_1\sinh\omega_\rho\hbar(\beta-t)}{\sinh\omega_\rho\hbar\beta})^2\\
&+\sum_{n=1}^{\infty}f(z_1,z_2)^n-\frac{\cosh(2\omega_\rho\hbar t-\omega_\rho\hbar\beta)}{\cosh\omega_\rho\hbar\beta}\sum_{n=1}^{\infty}f(z_1,z_2)^n\\
&+\frac{2m\omega_\rho}{\hbar\coth\omega_\rho\hbar\beta}(\frac{x_2\sinh\omega_\rho\hbar t+x_1\sinh\omega_\rho\hbar(\beta-t)}{\sinh\omega_\rho\hbar\beta})^2\sum_{n=1}^{\infty}f(z_1,z_2)^n].
\end{aligned} \tag{4.38}$$

Considering the integral of the first term $\int_0^\beta \frac{\omega_z\hbar\coth\omega_\rho\hbar\beta}{\omega_\rho(\gamma\hbar\coth\omega_z\hbar\beta+2m\omega_z\theta)}dt$, If we take limit $\beta\to\infty$ at very low temperatures, then $\coth\omega_\rho\hbar\beta\to 1$ and so

$$\int_0^\beta \frac{\omega_z\hbar\coth\omega_\rho\hbar\beta}{\omega_\rho\left(\gamma\hbar\coth\omega_z\hbar\beta+2m\omega_z\theta\right)}dt=\frac{\omega_z\hbar\beta}{\omega_\rho\left(\gamma\hbar+2m\omega_z\theta\right)}. \tag{4.39}$$

On the other hand if we expand $\coth\omega_\rho\hbar\beta$ and $\coth\omega_z\hbar\beta$ by using the relation in Eq. (4.30), we find that $\frac{\omega_z\hbar\beta}{\omega_\rho(\gamma\hbar+2m\omega_z\theta)}$ is the leading term depending on β. We thus expand $\frac{1}{\cosh\omega_\rho\hbar\beta}$, $\frac{1}{\cosh\omega_z\hbar\beta}$, $\frac{1}{\sinh\omega_\rho\hbar\beta}$ and $\frac{1}{\sinh\omega_z\hbar\beta}$ using Eq. (4.30) and let $\coth\omega_\rho\hbar\beta\to 1$, Then it easy to integrate Eq. (4.38) since all terms are exponential functions. Retaining only the terms which depend on β and the terms of the lowest power of $e^{-\omega_\rho\hbar\beta}$ or $e^{-\omega_z\hbar\beta}$, in order to find energy and wave functions, we finally obtain

$$\begin{aligned}\int_0^\beta \frac{\langle x^2\rangle}{\gamma\langle z^2\rangle+\theta}dt &= \frac{\omega_z\hbar\beta}{\omega_\rho\left(\gamma\hbar+2m\omega_z\theta\right)}\\ &\quad+\frac{2m\omega_z}{\hbar\left(\gamma\hbar+2m\omega_z\theta\right)}\left(\frac{(x_1^2+x_2^2)}{2\omega_\rho}-x_1x_2e^{-\omega_\rho\hbar\beta}+\ldots\right)\\ &\quad-\frac{2\gamma m\omega_z^2}{\omega_\rho\left(\gamma\hbar+2m\omega_z\theta\right)^2}\left(\frac{(z_1^2+z_2^2)}{2\omega_z}-z_1z_2e^{-\omega_z\hbar\beta}+\ldots\right)\\ &\quad-\frac{4\gamma m^2\omega_z^2}{\left(\gamma\hbar+2m\omega_z\theta\right)^2}\left(\frac{(x_1^2z_1^2+x_2^2z_2^2)}{2(\omega_\rho+\omega_z)\hbar}+\ldots\right).\end{aligned} \tag{4.40}$$

Our next task is to calculate the average of Delta function. To do so, we first calculate the average of Delta function in real time. In order to manipulate the delta function within the path integral, we express it by its Fourier transform,

$$\begin{aligned}\langle\delta(\mathbf{r}_i-\mathbf{r}_j)\rangle_{S_0} &= \int_{-\infty}^{\infty}d\mathbf{k}\frac{1}{(2\pi)^3}\left\langle e^{i\mathbf{k}\cdot(\mathbf{r}_i-\mathbf{r}_j)}\right\rangle_{S_0}\\ &= \int_{-\infty}^{\infty}d\mathbf{k}_x\frac{1}{(2\pi)}\left\langle e^{i\mathbf{k}_x\cdot(\mathbf{x}_i-\mathbf{x}_j)}\right\rangle_{S_0}\int_{-\infty}^{\infty}d\mathbf{k}_y\frac{1}{(2\pi)}\left\langle e^{i\mathbf{K}_y\cdot(\mathbf{y}_i-\mathbf{y}_j)}\right\rangle_{S_0}\\ &\quad\times\int_{-\infty}^{\infty}d\mathbf{k}_z\frac{1}{(2\pi)}\left\langle e^{i\mathbf{k}_z\cdot(\mathbf{z}_i-\mathbf{z}_j)}\right\rangle_{S_0}\end{aligned} \tag{4.41}$$

Consider Eq.(4.41) in the x component only

$$\left\langle e^{i\mathbf{k}_x\cdot(\mathbf{x}_i-\mathbf{x}_j)}\right\rangle_{S_0} = \frac{\int_{r_1}^{r_2} Dx(t)e^{\frac{i}{\hbar}(S_0(x_i)+\hbar\mathbf{k}_x\cdot\mathbf{x}_i)}}{\int_{r_1}^{r_2} Dx(t)e^{\frac{i}{\hbar}S_0(x_i)}}\cdot\frac{\int_{r_1}^{r_2} Dx(t)e^{\frac{i}{\hbar}(S_0(x_j)-\hbar\mathbf{k}_x\cdot\mathbf{x}_j)}}{\int_{r_1}^{r_2} Dx(t)e^{\frac{i}{\hbar}S_0(x_j)}} \tag{4.42}$$

In the dominator, the exponent has the explicit form

$$S_0(x_i)+\hbar\mathbf{k}\cdot\mathbf{x}_i = \int_0^t dt(\frac{m}{2}\,\dot{x}_i^2 - \frac{m}{2}\omega^2 x_i^2 + f(t)x_i) \tag{4.43}$$

where $f(t)=\hbar\mathbf{k}_x\delta(t-s)$, so the kernel $K_{S_0(x_i)+\hbar\mathbf{k}\cdot\mathbf{x}_i}$ is

$$\begin{aligned}
&(\frac{m}{2\pi i\hbar\sin\omega T})^{1/2}\\
&\exp[\frac{m\omega i}{2\hbar\sin\omega T}(\cos\omega T(x_{i_2}^2+x_{i_1}^2)-2x_{i_2}x_{i_1}+\frac{2x_{i_2}}{m\omega}\hbar\mathbf{k}\sin\omega t\\
&+\frac{2x_{i_1}}{m\omega}\hbar\mathbf{k}\sin\omega(T-t)-\frac{1}{m^2\omega^2}\hbar^2\mathbf{k}^2\sin\omega(T-t)\sin\omega t)]\\
=\;& K_{S_0(x_i)}\exp\left[ix_{i_2}\mathbf{k}\frac{\sin\omega t}{\sin\omega T}+ix_{i_1}\mathbf{k}\frac{\sin\omega\,(T-t)}{\sin\omega T}-\frac{i\hbar\mathbf{k}^2}{2m\omega}\frac{\sin\omega\,(T-t)\sin\omega t}{\sin\omega T}\right]
\end{aligned} \tag{4.44}$$

where $K_{S_0(x_i)}$ is the kernel of harmonic oscillator. Similarly, we obtain

$$\begin{aligned}
K_{S_0(x_i)-\hbar kx_i} &= K_{S_0(x_i)}\exp[-ix_{i2}\mathbf{k}\frac{\sin\omega t}{\sin\omega T}-ix_{i1}\mathbf{k}\frac{\sin\omega\,(T-t)}{\sin\omega T}\\
&\quad -\frac{i\hbar\mathbf{k}^2}{2m\omega}\frac{\sin\omega\,(T-t)\sin\omega t}{\sin\omega T}].
\end{aligned} \tag{4.45}$$

Substituting Eq. (4.44) and Eq. (4.45) into Eq. (4.42), we get

$$\begin{aligned}
\left\langle e^{i\mathbf{k}_x\cdot(\mathbf{x}_i-\mathbf{x}_j)}\right\rangle_{S_0} &= \exp[\mathbf{k}\cdot\left(i(\mathbf{x}_{i_2}-\mathbf{x}_{j_2})\frac{\sin\omega t}{\sin\omega T}+i(\mathbf{x}_{i_1}-\mathbf{x}_{j_1})\frac{\sin\omega\,(T-t)}{\sin\omega T}\right)\\
&\quad -\mathbf{k}^2\frac{i\hbar}{2m\omega}\frac{\sin\omega\,(T-t)\sin\omega t}{\sin\omega T}].
\end{aligned} \tag{4.46}$$

Using the formula $\int_{-\infty}^{\infty} dxe^{-ax^2+bx}=\sqrt{\frac{\pi}{a}}e^{b^2/4a}$, we get

$$\int_{-\infty}^{\infty} d\mathbf{k}\frac{1}{2\pi}\left\langle e^{i\mathbf{k}_x\cdot(\mathbf{x}_i-\mathbf{x}_j)}\right\rangle_{S_0} = \left(\frac{m\pi\omega\sin\omega T}{i\hbar\sin\omega(T-t)\sin\omega t}\right)^{1/2}\times$$

$$\exp[\left(\frac{im\omega\sin\omega T}{4\hbar\sin\omega(T-t)\sin\omega t}\right) \times\left(\frac{(x_{i_2}-x_{j_2})\sin\omega t+(x_{i_1}-x_{j_1})\sin\omega\left(T-t\right)}{\sin\omega T}\right)^2]. \tag{4.47}$$

The y and z factor of Eq. (4.41) have a similar form. We thus obtain

$$\begin{aligned}\left\langle\delta(\mathbf{r}_i-\mathbf{r}_j)\right\rangle_{S_0} &= \frac{1}{(2\pi)^3}\left(\frac{m\pi\omega_\rho\sin\omega_\rho T}{i\hbar\sin\omega_\rho(T-t)\sin\omega_\rho t}\right)\left(\frac{m\pi\omega_z\sin\omega_z T}{i\hbar\sin\omega_z(T-t)\sin\omega_z t}\right)^{1/2} \\ &\exp[(\frac{im\omega_\rho\left((x_{i_2}-x_{j_2})\sin\omega t+(x_{i_1}-x_{j_1})\sin\omega\left(T-t\right)\right)^2}{4\hbar\sin\omega(T-t)\sin\omega t\sin\omega T} \\ &+\frac{im\omega_\rho\left((y_{i_2}-y_{j_2})\sin\omega_\rho t+(y_{i_1}-y_{j_1})\sin\omega_\rho\left(T-t\right)\right)^2}{4\hbar\sin\omega_\rho(T-t)\sin\omega_\rho t\sin\omega_\rho T} \\ &+\frac{im\omega_z\left((z_{i_2}-z_{j_2})\sin\omega_z t+(z_{i_1}-z_{j_1})\sin\omega_z\left(T-t\right)\right)^2}{4\hbar\sin\omega_z(T-t)\sin\omega_z t\sin\omega_z T})].\end{aligned} \tag{4.48}$$

Changing real time to imaginary time in Eq. (4.48), we get

$$\begin{aligned}\left\langle\delta(r_i-r_j)\right\rangle_{S_0} &= \left(\frac{m\omega_\rho\sinh\omega_\rho\hbar\beta}{4\pi\hbar\sinh\omega_\rho\hbar(\beta-t)\sinh\omega_\rho\hbar t}\right)\left(\frac{m\pi\omega_z\sin\omega_z\hbar\beta}{4\hbar\sin\omega_z\hbar(\beta-t)\sin\omega_z\hbar t}\right)^{1/2} \\ &\times\exp[(\frac{m\omega_\rho\left((x_{i_2}-x_{j_2})\sinh\omega\hbar t+(x_{i_1}-x_{j_1})\sinh\omega\hbar\left(\beta-t\right)\right)^2}{4\hbar\sinh\omega\hbar(\beta-t)\sinh\omega\hbar t\sinh\omega\hbar\beta} \\ &+\frac{m\omega_\rho\left((y_{i_2}-y_{j_2})\sinh\omega_\rho\hbar t+(y_{i_1}-y_{j_1})\sinh\omega_\rho\hbar\left(\beta-t\right)\right)^2}{4\hbar\sinh\omega_\rho\hbar(\beta-t)\sinh\omega_\rho\hbar t\sinh\omega_\rho\hbar\beta} \\ &+\frac{m\omega_z\left((z_{i_2}-z_{j_2})\sinh\omega_z\hbar t+(z_{i_1}-z_{j_1})\sinh\omega_z\hbar\left(\beta-t\right)\right)^2}{4\hbar\sinh\omega_z\hbar(\beta-t)\sinh\omega_z\hbar t\sinh\omega_z\hbar\beta})].\end{aligned} \tag{4.49}$$

Using the relation

$$e^x=\sum_{n=0}^{\infty}\frac{x^n}{n!}=1+x+\frac{1}{2}x^2+\frac{1}{6}x^3+... \tag{4.50}$$

We can write $\left\langle\delta(\mathbf{r}_i-\mathbf{r}_j)\right\rangle_{S_0}$ as

$$\left(\frac{m\omega_\rho\sinh\omega_\rho\hbar\beta}{4\pi\hbar\sinh\omega_\rho\hbar(\beta-t)\sinh\omega_\rho\hbar t}\right)\left(\frac{m\pi\omega_z\sinh\omega_z\hbar\beta}{4\hbar\sin\omega_z\hbar(\beta-t)\sin\omega_z\hbar t}\right)^{1/2}$$

$$\times \left(\begin{array}{l} 1+\left(\begin{array}{l} \frac{m\omega_\rho\left((x_{i_2}-x_{j_2})\sinh\omega\hbar t+(x_{i_1}-x_{j_1})\sinh\omega\hbar(\beta-t)\right)^2}{4\hbar\sinh\omega\hbar(\beta-t)\sinh\omega\hbar t\sinh\omega\hbar\beta} \\ +\frac{m\omega_\rho\left((y_{i_2}-y_{j_2})\sinh\omega_\rho\hbar t+(y_{i_1}-y_{j_1})\sinh\omega_\rho\hbar(\beta-t)\right)^2}{4\hbar\sinh\omega_\rho\hbar(\beta-t)\sinh\omega_\rho\hbar t\sinh\omega_\rho\hbar\beta} \\ +\frac{m\omega_z\left((z_{i_2}-z_{j_2})\sinh\omega_z\hbar t+(z_{i_1}-z_{j_1})\sinh\omega_z\hbar(\beta-t)\right)^2}{4\hbar\sinh\omega_z\hbar(\beta-t)\sinh\omega_z\hbar t\sinh\omega_z\hbar\beta} \end{array} \right) \\ +\frac{1}{2}\left(\begin{array}{l} \frac{m\omega_\rho\left((x_{i_2}-x_{j_2})\sinh\omega\hbar t+(x_{i_1}-x_{j_1})\sinh\omega\hbar(\beta-t)\right)^2}{4\hbar\sinh\omega\hbar(\beta-t)\sinh\omega\hbar t\sinh\omega\hbar\beta} \\ +\frac{m\omega_\rho\left((y_{i_2}-y_{j_2})\sinh\omega_\rho\hbar t+(y_{i_1}-y_{j_1})\sinh\omega_\rho\hbar(\beta-t)\right)^2}{4\hbar\sinh\omega_\rho\hbar(\beta-t)\sinh\omega_\rho\hbar t\sinh\omega_\rho\hbar\beta} \\ +\frac{m\omega_z\left((z_{i_2}-z_{j_2})\sinh\omega_z\hbar t+(z_{i_1}-z_{j_1})\sinh\omega_z\hbar(\beta-t)\right)^2}{4\hbar\sinh\omega_z\hbar(\beta-t)\sinh\omega_z\hbar t\sinh\omega_z\hbar\beta} \end{array} \right)^2 + \ldots \end{array} \right). \quad (4.51)$$

Considering the first term and using the relation from Eq. (4.36), we can write

$$\begin{aligned} & \left(\frac{m\omega_\rho\sinh\omega_\rho\hbar\beta}{4\pi\hbar\sinh\omega_\rho\hbar(\beta-t)\sinh\omega_\rho\hbar t}\right)\left(\frac{m\pi\omega_z\sin\omega_z\hbar\beta}{4\hbar\sin\omega_z\hbar(\beta-t)\sin\omega_z\hbar t}\right)^{1/2} \\ = & \left(\frac{m\omega_\rho}{2\pi\hbar}\frac{\sinh\omega_\rho\hbar\beta}{\cosh\omega_\rho\hbar\beta}\frac{1}{\left(1-\frac{\cosh(2\omega_\rho\hbar t-\omega_\rho\hbar\beta)}{\cosh\omega_\rho\hbar\beta}\right)}\right) \\ & \left(\frac{m\omega_z}{2\pi\hbar}\frac{\sinh\omega_z\hbar\beta}{\cosh\omega_z\hbar\beta}\frac{1}{\left(1-\frac{\cosh(2\omega_z\hbar t-\omega_z\hbar\beta)}{\cosh\omega_z\hbar\beta}\right)}\right)^{1/2}. \end{aligned} \quad (4.52)$$

and the relation

$$\frac{1}{\sqrt{(1-x)}} = \sum_{n=0}^{\infty}\binom{-\frac{1}{2}}{n}(-x)^n = 1+\frac{1}{2}x+\frac{3}{8}x^2+\frac{5}{16}x^3+\ldots \quad (4.53)$$

where $\binom{k}{n} = \frac{k(k-1)\cdots(k-n+1)}{n!}$. We can write the right-hand side of Eq. (4.52) as

$$\begin{aligned} & \left(\frac{m\omega_\rho}{2\pi\hbar}\frac{\sinh\omega_\rho\hbar\beta}{\cosh\omega_\rho\hbar\beta}\right)\left(\frac{m\omega_z}{2\pi\hbar}\frac{\sinh\omega_z\hbar\beta}{\cosh\omega_z\hbar\beta}\right)^{1/2} \\ & \times\left(1+\sum_{n=1}^{\infty}\left(\frac{\cosh(2\omega_\rho\hbar t-\omega_\rho\hbar\beta)}{\cosh\omega_\rho\hbar\beta}\right)^n\right) \\ & \times\left(1+\sum_{n=1}^{\infty}\binom{-\frac{1}{2}}{n}\left(\frac{\cosh(2\omega_z\hbar t-\omega_z\hbar\beta)}{\cosh\omega_z\hbar\beta}\right)^n\right). \end{aligned} \quad (4.54)$$

Integrating Eq.(4.54), we get

$$\int_0^\beta\left(\frac{m\omega_\rho}{2\pi\hbar}\tanh\omega_\rho\hbar\beta\right)\left(\frac{m\omega_z}{2\pi\hbar}\tanh\omega_z\hbar\beta\right)^{1/2}$$

$$\times \left(\begin{array}{c} 1+\sum\limits_{n=1}^{\infty}\left(\frac{\cosh(2\omega_\rho\hbar t-\omega_\rho\hbar\beta)}{\cosh\omega_\rho\hbar\beta}\right)^n+\sum\limits_{n=1}^{\infty}\binom{-\frac{1}{2}}{n}\left(\frac{\cosh(2\omega_z\hbar t-\omega_z\hbar\beta)}{\cosh\omega_z\hbar\beta}\right)^n \\ +\sum\limits_{n=1}^{\infty}\left(\frac{\cosh(2\omega_\rho\hbar t-\omega_\rho\hbar\beta)}{\cosh\omega_\rho\hbar\beta}\right)^n\sum\limits_{n=1}^{\infty}\binom{-\frac{1}{2}}{n}\left(\frac{\cosh(2\omega_z\hbar t-\omega_z\hbar\beta)}{\cosh\omega_z\hbar\beta}\right)^n \end{array} \right) dt \tag{4.55}$$

Considering the summation terms, the results of integration are exponential functions and constants. We are interested only in the first term because the result from integration depends on β. Expanding $\tanh\omega_\rho\hbar\beta$ and $\tanh\omega_z\hbar\beta$ as a power series, we can rewrite Eq. (4.55) as

$$\begin{aligned} &\int_0^\beta \left(\frac{m\omega_\rho}{2\pi\hbar}\tanh\omega_\rho\hbar\beta\right)\left(\frac{m\omega_z}{2\pi\hbar}\tanh\omega_z\hbar\beta\right)^{1/2} \\ &\times \left(\begin{array}{c} 1+\sum\limits_{n=1}^{\infty}\left(\frac{\cosh(2\omega_\rho\hbar t-\omega_\rho\hbar\beta)}{\cosh\omega_\rho\hbar\beta}\right)^n+\sum\limits_{n=1}^{\infty}\binom{-\frac{1}{2}}{n}\left(\frac{\cosh(2\omega_z\hbar t-\omega_z\hbar\beta)}{\cosh\omega_z\hbar\beta}\right)^n \\ +\sum\limits_{n=1}^{\infty}\left(\frac{\cosh(2\omega_\rho\hbar t-\omega_\rho\hbar\beta)}{\cosh\omega_\rho\hbar\beta}\right)^n\sum\limits_{n=1}^{\infty}\binom{-\frac{1}{2}}{n}\left(\frac{\cosh(2\omega_z\hbar t-\omega_z\hbar\beta)}{\cosh\omega_z\hbar\beta}\right)^n \end{array} \right) dt \\ =\ &\left(\frac{m\omega_\rho}{2\pi\hbar}\right)\left(\frac{m\omega_z}{2\pi\hbar}\right)^{1/2}\beta\tanh\omega_\rho\hbar\beta\left(\tanh\omega_z\hbar\beta\right)^{1/2}+... \\ =\ &\left(\frac{m\omega_\rho}{2\pi\hbar}\right)\left(\frac{m\omega_z}{2\pi\hbar}\right)^{1/2}\beta\left(1+2e^{-2\omega_\rho\hbar\beta}+e^{-2\omega_z\hbar\beta}+e^{-(4\omega_\rho+2\omega_z)\hbar\beta}+...\right)+... \end{aligned} \tag{4.56}$$

Next, we consider the next integral of the term of the delta function in Eq. (4.51),

$$\begin{aligned} &\int_0^\beta \left(\frac{m\omega_\rho\sinh\omega_\rho\hbar\beta}{4\pi\hbar\sinh\omega_\rho\hbar(\beta-t)\sinh\omega_\rho\hbar t}\right)\left(\frac{m\pi\omega_z\sinh\omega_z\hbar\beta}{4\hbar\sin\omega_z\hbar(\beta-t)\sin\omega_z\hbar t}\right) \\ &\times\Big(\frac{m\omega_\rho\left((x_{i2}-x_{j2})\sinh\omega_\rho\hbar t+(x_{i1}-x_{j1})\sinh\omega_\rho\hbar\left(\beta-t\right)\right)^2}{4\hbar\sinh\omega_\rho\hbar(\beta-t)\sinh\omega_\rho\hbar t\sinh\omega_\rho\hbar\beta} \\ &+\frac{m\omega_\rho\left((y_{i2}-y_{j2})\sinh\omega_\rho\hbar t+(y_{i1}-y_{j1})\sinh\omega_\rho\hbar\left(\beta-t\right)\right)^2}{4\hbar\sinh\omega_\rho\hbar(\beta-t)\sinh\omega_\rho\hbar t\sinh\omega_\rho\hbar\beta} \\ &+\frac{m\omega_z\left((z_{i2}-z_{j2})\sinh\omega_z\hbar t+(z_{i1}-z_{j1})\sinh\omega_z\hbar\left(\beta-t\right)\right)^2}{4\hbar\sinh\omega_z\hbar(\beta-t)\sinh\omega_z\hbar t\sinh\omega_z\hbar\beta}\Big)dt \end{aligned} \tag{4.57}$$

To simplify this equation, we use only the leading term of the first factor shown in Eq. (4.55) because we need to find the lowest power of the exponentials $e^{-\omega_\rho\hbar\beta}$

and $e^{-\omega_z\hbar\beta}$. Thus we may write the term in (4.57) as

$$\begin{aligned}
&\left(\frac{m\omega_\rho}{2\pi\hbar}\right)\left(\frac{m\omega_z}{2\pi\hbar}\right)^{1/2} \\
&\times(\int_0^\beta\left(\frac{m\omega_\rho\left((x_{i2}-x_{j2})\sinh\omega_\rho\hbar t+(x_{i1}-x_{j1})\sinh\omega_\rho\hbar\left(\beta-t\right)\right)^2}{4\hbar\sinh\omega_\rho\hbar(\beta-t)\sinh\omega_\rho\hbar t\sinh\omega_\rho\hbar\beta}\right)dt \\
&+\int_0^\beta\left(\frac{m\omega_\rho\left((y_{i2}-y_{j2})\sinh\omega_\rho\hbar t+(y_{i1}-y_{j1})\sinh\omega_\rho\hbar\left(\beta-t\right)\right)^2}{4\hbar\sinh\omega_\rho\hbar(\beta-t)\sinh\omega_\rho\hbar t\sinh\omega_\rho\hbar\beta}\right)dt \\
&+\int_0^\beta\left(\frac{m\omega_z\left((z_{i2}-z_{j2})\sinh\omega_z\hbar t+(z_{i1}-z_{j1})\sinh\omega_z\hbar\left(\beta-t\right)\right)^2}{4\hbar\sinh\omega_z\hbar(\beta-t)\sinh\omega_z\hbar t\sinh\omega_z\hbar\beta}\right)dt).
\end{aligned} \tag{4.58}$$

Consider the first term of (4.58)

$$\begin{aligned}
&\int_0^\beta\left(\frac{m\omega_\rho\left((x_{i2}-x_{j2})\sinh\omega_\rho\hbar t+(x_{i1}-x_{j1})\sinh\omega_\rho\hbar\left(\beta-t\right)\right)^2}{4\hbar\sinh\omega_\rho\hbar(\beta-t)\sinh\omega_\rho\hbar t\sinh\omega_\rho\hbar\beta}\right)dt \\
=&\int_0^\beta\frac{m\omega_\rho\left[(x_{i2}-x_{j2})\sinh\omega_\rho\hbar t+(x_{i1}-x_{j1})\sinh\omega_\rho\hbar\left(\beta-t\right)\right]^2}{2\hbar\sinh\omega_\rho\hbar\beta\left(\cosh\omega_\rho\hbar\beta-\cosh(2\omega_\rho\hbar t-\omega_\rho\hbar\beta)\right)} \\
=&\int_0^\beta\frac{m\omega_\rho}{2\hbar\sinh\omega_\rho\hbar\beta\cosh\omega_\rho\hbar\beta}\frac{\left((x_{i2}-x_{j2})\sinh\omega_\rho\hbar t+(x_{i1}-x_{j1})\sinh\omega_\rho\hbar\left(\beta-t\right)\right)^2}{\left(1-\frac{\cosh(2\omega_\rho\hbar t-\omega_\rho\hbar\beta)}{\cosh\omega_\rho\hbar\beta}\right)} \\
&\int_0^\beta\frac{m\omega_\rho}{2\hbar\sinh\omega_\rho\hbar\beta\cosh\omega_\rho\hbar\beta}\left((x_{i2}-x_{j2})\sinh\omega_\rho\hbar t+(x_{i1}-x_{j1})\sinh\omega_\rho\hbar\left(\beta-t\right)\right)^2 \\
&\times\left(1+\sum_{n=1}^\infty\left(\frac{\cosh(2\omega_\rho\hbar t-\omega_\rho\hbar\beta)}{\cosh\omega_\rho\hbar\beta}\right)^n\right)dt \\
=&\frac{m}{4\hbar^2}(x_{i_1}^2+x_{j_1}^2+x_{i_2}^2+x_{j_2}^2)-\frac{m}{2\hbar^2}(x_{i_1}-x_{j_1})(x_{i_2}-x_{j_2})e^{-\omega_\rho\hbar\beta}+...
\end{aligned} \tag{4.59}$$

Substituting (4.59) into (4.57), we obtain

$$\begin{aligned}
\int_0^\beta\langle\delta(\mathbf{r}_i-\mathbf{r}_j)\rangle\,dt &= \left(\frac{m\omega_\rho}{2\pi\hbar}\right)\left(\frac{m\omega_z}{2\pi\hbar}\right)^{1/2}\beta\left(1+2e^{-\omega_\rho\hbar\beta}+e^{-\omega_z\hbar\beta}+...\right) \\
&\quad+\left(\frac{m\omega_\rho}{2\pi\hbar}\right)\left(\frac{m\omega_z}{2\pi\hbar}\right)^{1/2}\left(\frac{m}{4\hbar^2}(x_{i_1}^2+x_{j_1}^2+x_{i_2}^2+x_{j_2}^2)\right)
\end{aligned}$$

$$+\left(\frac{m\omega_\rho}{2\pi\hbar}\right)\left(\frac{m\omega_z}{2\pi\hbar}\right)^{1/2}\left(\frac{m}{4\hbar^2}(y_{i_1}^2+y_{j_1}^2+y_{i_2}^2+y_{j_2}^2)\right)$$
$$+\left(\frac{m\omega_\rho}{2\pi\hbar}\right)\left(\frac{m\omega_z}{2\pi\hbar}\right)^{1/2}\left(\frac{m}{4\hbar^2}(z_{i_1}^2+z_{j_1}^2+z_{i_2}^2+z_{j_2}^2)\right)$$
$$+... \tag{4.60}$$

Having evaluated all terms in the exponent of Eq. (4.17), we now find the density matrix of a harmonic oscillator ρ_0 of N particles. First, consider the kernel of a one dimensional harmonic oscillator that has been worked out in Chapter 2, that is

$$K(\mathbf{x}_2,T;\mathbf{x}_1,0) = \left(\frac{m\omega_\rho}{2\pi i\hbar\sin\omega_\rho T}\right)^{1/2} \exp\left(\frac{im\omega_\rho}{2\hbar\sin\omega_\rho T}\right)\left[\left(x_1^2+x_2^2\right)\cos\omega_\rho T-2x_1x_2\right]. \tag{4.61}$$

If the time of the kernel is replaced by $-i\beta\hbar$ so that $\sin(-i\omega_\rho\beta\hbar)=-i\sinh\omega_\rho\beta\hbar$ and $\cos(-i\omega_\rho\beta\hbar)=\cosh\omega_\rho\beta\hbar$, then we obtain the expression for the density matrix,

$$\rho(\mathbf{x}_2,\beta;\mathbf{x}_1,0) = \left(\frac{m\omega_\rho}{2\pi\hbar\sinh\omega_\rho\beta\hbar}\right)^{1/2} \exp\left(-\frac{m\omega_\rho}{2\hbar\sinh\omega_\rho\beta\hbar}\right)\left[\left(x_1^2+x_2^2\right)\cosh\omega_\rho\beta\hbar-2x_1x_2\right]. \tag{4.62}$$

Using the relations

$$\sinh\omega_\rho\beta\hbar = \frac{1}{2e^{\omega_\rho\beta\hbar}\left(1-e^{-2\omega_\rho\beta\hbar}\right)}$$
$$\cosh\omega_\rho\beta\hbar = \frac{1}{2e^{\omega_\rho\beta\hbar}\left(1+e^{-2\omega_\rho\beta\hbar}\right)} \tag{4.63}$$

We can write $\rho(\mathbf{x}_2,\beta;\mathbf{x}_1,0)$ as

$$\left(\frac{m\omega_\rho}{\pi\hbar}\right)^{1/2}e^{-\omega_\rho\beta\hbar/2}\left(1-e^{-2\omega_\rho\beta\hbar}\right)^{-1/2}$$

$$\times \exp\left\{\left(-\frac{Nm\omega_\rho}{2\hbar}\right)\left[\left(x_1^2+x_2^2\right)\frac{\left(1+e^{-2\omega_\rho\beta\hbar}\right)}{\left(1-e^{-2\omega_\rho\beta\hbar}\right)}-\left(\frac{4x_1x_2e^{-\omega_\rho\beta\hbar}}{\left(1-e^{-2\omega_\rho\beta\hbar}\right)}\right)\right]\right\}. \tag{4.64}$$

Expanding the right-hand side of Eq. (4.62), we obtain the density matrix of a one-dimensional harmonic oscillator in a series form,

$$\begin{aligned}&\left(\frac{m\omega_\rho}{\pi\hbar}\right)^{1/2}e^{-\frac{m\omega_\rho}{2\hbar}\left(x_1^2+x_2^2\right)}e^{-\omega_\rho\beta\hbar/2}\left(1+\frac{1}{2}e^{-2\omega_\rho\beta\hbar}+...\right)\\&\times\left[1+\frac{2m\omega_\rho}{\hbar}x_1x_2e^{-\omega_\rho\beta\hbar}-\frac{m\omega_\rho}{\hbar}\left(x_1^2+x_2^2\right)e^{-2\omega_\rho\beta\hbar}+...\right]\end{aligned} \tag{4.65}$$

The above result can be generalized to a three-dimensional case as

$$\begin{aligned}&\rho(\mathbf{r}_2,\beta;\mathbf{r}_1,0)=\left(\frac{m\omega_\rho}{\pi\hbar}\right)\left(\frac{m\omega_z}{\pi\hbar}\right)^{1/2}e^{-\frac{m\omega_\rho}{2\hbar}\left(x_1^2+x_2^2+y_1^2+y_2^2\right)}e^{-\frac{m\omega_z}{2\hbar}\left(z_1^2+z_2^2\right)}e^{-(\omega_\rho\beta\hbar+\omega_z\beta\hbar/2)}\\&\left[1+\frac{2m\omega_\rho}{\hbar}x_1x_2e^{-\omega_\rho\beta\hbar}-\frac{m\omega_\rho}{\hbar}\left(x_1^2+x_2^2\right)e^{-2\omega_\rho\beta\hbar}+...\right]\\&\left[1+\frac{2m\omega_\rho}{\hbar}y_1y_2e^{-\omega_\rho\beta\hbar}-\frac{m\omega_\rho}{\hbar}\left(y_1^2+y_2^2\right)e^{-2\omega_\rho\beta\hbar}+...\right]\\&\left[1+\frac{2m\omega_z}{\hbar}z_1z_2e^{-\omega_z\beta\hbar}-\frac{m\omega_z}{\hbar}\left(z_1^2+z_2^2\right)e^{-2\omega_z\beta\hbar}+...\right]+...\end{aligned} \tag{4.66}$$

For a system of N three-dimensional harmonic oscillators, the density matrix is just the product of N one-particle density matrices of the form (4.67).

In the case of Bose-Einstein condensation in which all particles are confined in a small region, we may make the assumption that all particles are approximately at the same point in space. We therefore set $x_{i_1}=x_1$, $x_{i_2}=x_2$ for all $i=1,...,N$ and the same for y and z coordinates. Using Eq. (4.31) Eq. (4.40) Eq. (4.56) Eq. (4.60) and Eq. (4.66) together with this assumption in Eq. (4.17), we obtain our approximated result for the density matrix of the system of

N particles undergoing Bose-Einstein condensation in the Ioffe-Pritchard trap,

$$\begin{aligned}
\rho = & \left(\frac{m\omega_\rho}{\pi\hbar}\right)^N \left(\frac{m\omega_z}{\pi\hbar}\right)^{N/2} \exp\left[\begin{array}{c} -\frac{Nm\omega_\rho}{4\hbar}\left(x_1^2+x_2^2+y_1^2+y_2^2\right) \\ -\frac{Nm\omega_z}{4\hbar}\left(z_1^2+z_2^2\right)-\frac{N\gamma}{2\omega_z\hbar}(z_1^2+z_2^2) \\ -\frac{N\alpha^2 m\omega_z}{2\hbar\omega_\rho(\gamma\hbar+2m\omega_z\theta)}(x_1^2+x_2^2+y_1^2+y_2^2) \\ -\frac{N(N-1)}{2}\pi a\left(\frac{m\omega_\rho}{2\pi\hbar}\right)\left(\frac{m\omega_z}{2\pi\hbar}\right)^{1/2}\left(\begin{array}{c} x_1^2+x_2^2+y_1^2+y_2^2 \\ +z_1^2+z_2^2 \end{array}\right) \end{array}\right] \\
& \times \exp\left[-N\left(\begin{array}{c} \frac{1}{2}\omega_\rho\hbar+\frac{1}{4}\hbar\omega_z+\frac{\hbar}{2m\omega_z}\gamma+\frac{\alpha^2\omega_z\hbar}{\omega_\rho(\gamma\hbar+2m\omega_z\theta)} \\ +a\hbar\left(N-1\right)\sqrt{\frac{m}{2\pi\hbar}}\omega_\rho\sqrt{\omega_z} \end{array}\right)\beta\right] \\
& \times\left[1+\frac{2Nm\omega_\rho}{\hbar}x_1x_2e^{-\omega_\rho\beta\hbar}-\frac{Nm\omega_\rho}{\hbar}\left(x_1^2+x_2^2\right)e^{-2\omega_\rho\beta\hbar}+...\right] \\
& \times\left[1+\frac{2Nm\omega_\rho}{\hbar}y_1y_2e^{-\omega_\rho\beta\hbar}-\frac{Nm\omega_\rho}{\hbar}\left(y_1^2+y_2^2\right)e^{-2\omega_\rho\beta\hbar}+...\right] \\
& \times\left[1+\frac{2Nm\omega_z}{\hbar}z_1z_2e^{-\omega_z\beta\hbar}-\frac{Nm\omega_z}{\hbar}\left(z_1^2+z_2^2\right)e^{-2\omega_z\beta\hbar}+...\right] \\
& \times[1-\frac{Nm\omega_\rho}{2\hbar}x_1x_2e^{-\omega_\rho\hbar\beta}+\frac{Nm\omega_\rho}{2\hbar}(x_1+x_2)^2e^{-2\omega_\rho\hbar\beta} \\
& -\frac{Nm\omega_\rho}{2\hbar}y_1y_2e^{-\omega_\rho\hbar\beta}+\frac{Nm\omega_\rho}{2\hbar}(y_1+y_2)^2e^{-2\omega_\rho\hbar\beta}-\frac{Nm\omega_z}{2\hbar}z_1z_2e^{-\omega_z\hbar\beta} \\
& +\frac{N\gamma z_1z_2}{\omega_z\hbar}e^{-\omega_z\hbar\beta}-\frac{N\gamma(z_1+z_2)^2}{\omega_z\hbar}e^{-2\omega_z\hbar\beta}+\frac{N\alpha^2m\omega_zx_1x_2}{(\gamma\hbar+2m\omega_z\theta)}e^{-\omega_\rho\hbar\beta} \\
& +\frac{N\alpha^2m\omega_zy_1y_2}{(\gamma\hbar+2m\omega_z\theta)}e^{-\omega_\rho\hbar\beta}+\frac{N\alpha^2\gamma\hbar m\omega_z^2(z_1^2+z_2^2)}{\omega_\rho\omega_z\left(\gamma\hbar+2m\omega_z\theta\right)^2}-\frac{2N\alpha^2\gamma\hbar m\omega_z^2z_1z_2}{\omega_\rho\left(\gamma\hbar+2m\omega_z\theta\right)^2}e^{-\omega_z\hbar\beta}] \\
& +... \qquad (4.67)
\end{aligned}$$

From this result, we can pick out the coefficient of the lowest order term

$$e^{-E_0\beta}\phi_0(x_2)\phi_0^*(x_1)$$

$$\begin{aligned}
= & \left(\frac{m\omega_\rho}{\pi\hbar}\right)^N \left(\frac{m\omega_z}{\pi\hbar}\right)^{N/2} \exp\left[\begin{array}{c} -\frac{Nm\omega_\rho}{4\hbar}\left(x_1^2+x_2^2+y_1^2+y_2^2\right) \\ -\frac{Nm\omega_z}{4\hbar}\left(z_1^2+z_2^2\right)-\frac{N\gamma}{2\omega_z\hbar}(z_1^2+z_2^2) \\ -\frac{N\alpha^2 m\omega_z}{2\hbar\omega_\rho(\gamma\hbar+2m\omega_z\theta)}(x_1^2+x_2^2+y_1^2+y_2^2) \\ -\frac{N(N-1)}{2}\pi a\left(\frac{m\omega_\rho}{2\pi\hbar}\right)\left(\frac{m\omega_z}{2\pi\hbar}\right)^{1/2}\left(\begin{array}{c} x_1^2+x_2^2+y_1^2+y_2^2 \\ +z_1^2+z_2^2 \end{array}\right) \end{array}\right] \\
& \times \exp\left[-N\left(\begin{array}{c} \frac{1}{2}\omega_\rho\hbar+\frac{1}{4}\hbar\omega_z+\frac{\hbar}{2m\omega_z}\gamma+\frac{\alpha^2\omega_z\hbar}{\omega_\rho(\gamma\hbar+2m\omega_z\theta)} \\ +a\hbar\left(N-1\right)\sqrt{\frac{m}{2\pi\hbar}}\omega_\rho\sqrt{\omega_z} \end{array}\right)\beta\right] \qquad (4.68)
\end{aligned}$$

which means that the ground state energy of the entire system is approximatly

$$E_0 = N\left(\frac{1}{2}\omega_\rho\hbar + \frac{1}{4}\omega_z\hbar + \frac{\hbar\gamma}{2\omega_z m} + \frac{\alpha^2\hbar\omega_z}{\omega_\rho(\hbar\gamma + 2m\omega_z\theta)} + a\,(N-1)\,\hbar\sqrt{\frac{m}{2\pi\hbar}}\omega_\rho\sqrt{\omega_z}\right) \tag{4.69}$$

and the ground state wave function is roughly of the form

$$\begin{aligned}\phi_0(\mathbf{r}) &= \left(\frac{m\omega_\rho}{\pi\hbar}\right)^{N/2}\left(\frac{m\omega_z}{\pi\hbar}\right)^{N/4} \\ &\exp\left[-\frac{mN}{2\hbar}(\left(\frac{\omega_\rho}{2} + \frac{\alpha^2\omega_z}{\omega_\rho\,(\gamma\hbar + 2m\omega_z\theta)} + \frac{(N-1)}{2}a\sqrt{\frac{m}{2\pi\hbar}}\omega_\rho\sqrt{\omega_z}\right)\left(x^2+y^2\right)\right] \\ &\exp\left[-\frac{mN}{2\hbar}\left(\frac{\omega_z}{2} + \frac{\gamma}{m\omega_z} + \frac{(N-1)}{2}a\sqrt{\frac{m}{2\pi\hbar}}\omega_\rho\sqrt{\omega_z}\right)z^2)\right]\end{aligned} \tag{4.70}$$

where all particles are assumed to be located at the same point (x, y, z) in space. And noting that it is still unnormalized, we now normalize it by requiring that the wave function satisfies

$$\int_{-\infty}^{\infty}\phi_0(\mathbf{r})^*\phi_0(\mathbf{r})d^3\mathbf{r} = N. \tag{4.71}$$

The result is

$$\begin{aligned}\phi_0(\mathbf{r}) &= \sqrt{N}\left(\frac{Nm}{\pi\hbar}\left(\frac{\omega_\rho}{2} + \frac{\alpha^2\omega_z}{\omega_\rho\,(\gamma\hbar + 2m\omega_z\theta)} + \frac{(N-1)}{2}a\sqrt{\frac{m}{2\pi\hbar}}\omega_\rho\sqrt{\omega_z}\right)\right)^{N/2} \\ &\times\left(\frac{Nm}{\pi\hbar}\left(\frac{\omega_z}{2} + \frac{\gamma}{m\omega_z} + \frac{(N-1)}{2}a\sqrt{\frac{m}{2\pi\hbar}}\omega_\rho\sqrt{\omega_z}\right)\right)^{N/4} \\ &\times\exp\left[-\frac{Nm}{2\hbar}\left(\frac{\omega_\rho}{2} + \frac{\alpha^2\omega_z}{\omega_\rho\,(\gamma\hbar + 2m\omega_z\theta)} + \frac{(N-1)}{2}a\sqrt{\frac{m}{2\pi\hbar}}\omega_\rho\sqrt{\omega_z}\right)\rho^2\right] \\ &\times\exp\left[-\frac{Nm}{2\hbar}\left(\frac{\omega_z}{2} + \frac{\gamma}{m\omega_z} + \frac{(N-1)}{2}a\sqrt{\frac{m}{2\pi\hbar}}\omega_\rho\sqrt{\omega_z}\right)z^2\right].\end{aligned} \tag{4.72}$$

This is just a harmonic oscillator wave function with

$$\left(\frac{\omega_\rho}{2} + \frac{\alpha^2\omega_z}{\omega_\rho\,(\gamma\hbar + 2m\omega_z\theta)} + \frac{(N-1)}{2}a\sqrt{\frac{m}{2\pi\hbar}}\omega_\rho\sqrt{\omega_z}\right)$$

being a frequency in ρ direction and

$$\left(\frac{\omega_z}{2} + \frac{\gamma}{m\omega_z} + \frac{(N-1)}{2}a\sqrt{\frac{m}{2\pi\hbar}}\omega_\rho\sqrt{\omega_z}\right)$$

being a frequency in z direction of the entire system. We thus approximate the ground state energy and the wave function by Feynman's path integral theory. In the next chapter, we will analyse the physical meaning of these results and study the properties of Bose-Einstein condensation of atomic hydrogen.

สถาบันวิทยบริการ
จุฬาลงกรณ์มหาวิทยาลัย

Chapter 5

Numerical Analysis of the Results

In Chapter 4 we have calculated the ground state energy and the wave function of atomic hydrogen in an Ioffe-Pritchard trap. In this chapter we interpret the physical meaning of the results from Chapter 4 and compare these results to experiments. We address two topics. First, we calculate the ground state energy by a numerical method. The second topic is related to the ground state wave function, which tells us the size of the condensate cloud in the trap, the peak condensate density and other properties.

5.1 Minimization of Ground State Energy

In this section we minimize the approximated ground state energy function.

$$E(\omega_\rho, \omega_z) = N \left(\begin{array}{c} \frac{1}{2}\omega_\rho\hbar + \frac{1}{4}\omega_z\hbar + \frac{\hbar\gamma}{2\omega_z m} + \frac{\alpha^2\hbar\omega_z}{\omega_\rho(\hbar\gamma+2m\omega_z\theta)} \\ +a\,(N-1)\sqrt{\frac{m}{2\pi\hbar}}\omega_\rho\sqrt{\omega_z}\hbar \end{array} \right) \tag{5.1}$$

obtain in the previous chapter with respect to the effective frequencies, ω_ρ and ω_z, treated as variational parameters. The parameters α, γ and θ for the trap shape A are $\gamma = 25 \times k\ (J/cm^2)$, $\theta = 35 \times k\ (J)$ and $\alpha = 15.9 \times 10^3 \times k\ (J/cm)$. Condensates containing 1.2×10^9 atoms are observed in this trap. For hydrogen in ground state, $a = 0.648 \times 10^{-10}\ (m)$ which is repulsive for s-wave scattering length and mass of hydrogen is 1.6746×10^{-27} kg.

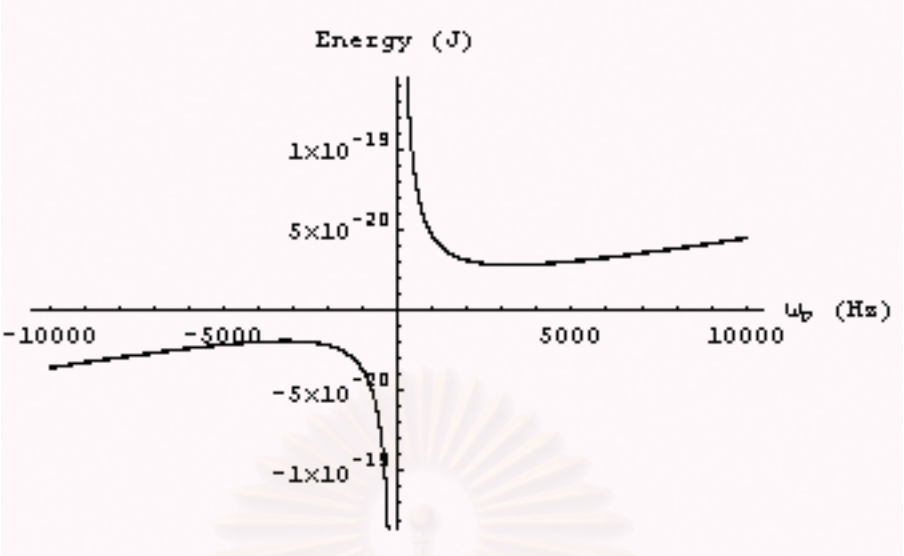

Figure 5.13: A plot showing energy vs ω_ρ.

We minimize the ground state energy by solving the partial derivative of $E(\omega_\rho, \omega_z)$ with respect to ω_ρ,

$$\frac{\partial}{\partial \omega_\rho} E(\omega_\rho, \omega_z) = 0. \tag{5.2}$$

and obtain

$$\omega_\rho = \pm \frac{\alpha \sqrt{2\omega_z} \pi^{1/4}}{\sqrt{\left(a\sqrt{\frac{2\omega_z m}{\hbar}} N + \sqrt{\pi}\right)(\gamma\hbar + 2\omega_z m\theta)}}. \tag{5.3}$$

If we fix the value of ω_z and vary ω_ρ, then we find two curves that have maximum and minimum points; in the case of ω_ρ being negative (positive) the curve has maximum (minimum) point (see Fig.(5.1)). And we fix the value of ω_ρ and vary ω_z, then we find one curves that have minimum point (see Fig.(5.1)).

Physically, the frequency can not be negative, thus we are interested only in the case of positive ω_ρ. Substituting $+\omega_\rho$ from Eq. (5.3) into Eq. (5.1), the

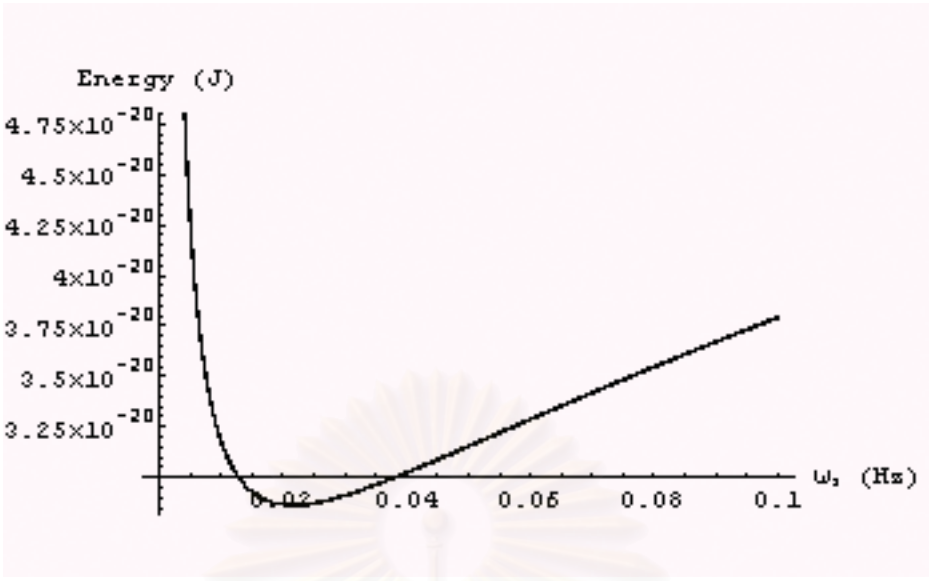

Figure 5.14: A plot showing energy vs ω_z.

ground state energy can be rewritten as

$$E(\omega_z) = N\hbar \left(\begin{array}{c} \frac{\alpha\sqrt{2\omega_z}\pi^{1/4}}{2\sqrt{\left(a\sqrt{\frac{2\omega_z m}{\hbar}}N+\sqrt{\pi}\right)(\gamma\hbar+2\omega_z m\theta)}} + \frac{1}{4}\omega_z + \frac{\gamma}{2\omega_z m} \\ + \frac{\alpha\sqrt{2\omega_z\left(a\sqrt{2}\sqrt{(\omega_z m\hbar)}N+\sqrt{\pi}\hbar\right)(\hbar\gamma+2m\omega_z\theta)\hbar}}{2\sqrt[4]{\pi}\hbar(\hbar\gamma+2m\omega_z\theta)} \\ + \frac{\sqrt{m}a(N-1)\alpha\omega_z}{\sqrt[4]{\pi}\sqrt{\left(a\sqrt{2}\sqrt{(\omega_z m\hbar)}N+\sqrt{\pi}\hbar\right)(\hbar\gamma+2m\omega_z\theta)}} \end{array} \right) \tag{5.4}$$

The energy function is now a function of one variable (ω_z). This function is very complicated and cannot be minimized by an analytical method. Therefore, we solve the problem numerically. In this thesis I use the Mathematica program to minimize the energy function, as also shown in Appendix A. We obtain the values; $\omega_\rho = 3787.54$ Hz, $\omega_z = 0.02686$ Hz and the ground state energy equal to $2.46751 \times 10^{-20} J$. We can also calculate the size of the condensate in an IP trap. Since the ground state wave function of BEC obtained in the previous chapter approximately has a form of the wave function of a harmonic oscillator. Thus we

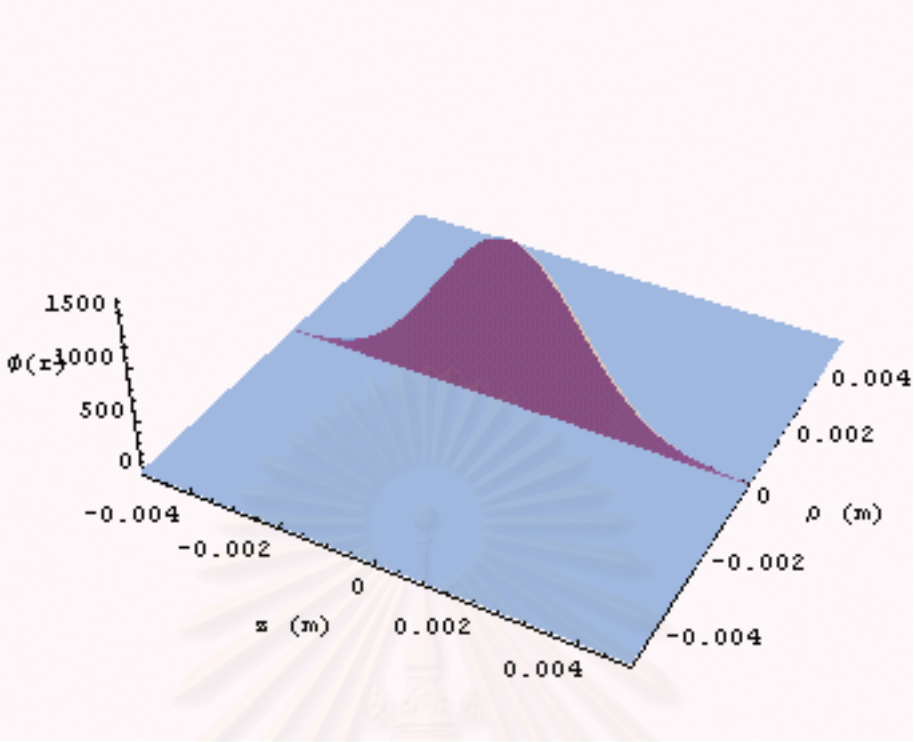

Figure 5.15: Ground state wave function plotted in 3 dimensions.

assume the ground state wave function as [23]

$$\phi(r) = N^{1/2}\left(\frac{m\omega_\rho}{\pi\hbar}\right)^{1/2}\left(\frac{m\omega_z}{\pi\hbar}\right)^{1/4}\exp\left[-\left(\frac{m\omega_\rho}{2\hbar}\rho^2+\frac{m\omega_z}{2\hbar}z^2\right)\right] \qquad (5.5)$$

with ω_ρ and ω_z having the values that minimize the energy function and treated as the effective frequencies of the entire system.

We plot $\phi(r)$ as a function ρ and z in 3 dimensions as shown in Fig. 5.2. This wave function is very thin in ρ direction and relatively very wide in z direction, so we can calculate the size of the condensate cloud in the trap from a Gaussian curve in Fig. 5.3.

The lengths of the condensate in respectively ρ and z direction are

$$\left(\frac{2\hbar}{m\omega_\rho}\right)^{1/2} = 5.8251\times10^{-6}\ m,$$

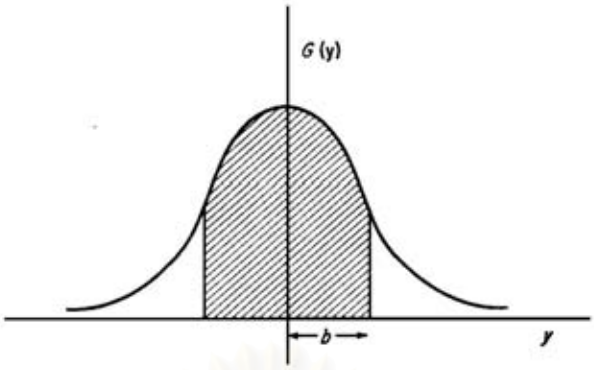

Figure 5.16: The form of the gaussian function $G(y) = e^{-y^2/2b^2}$, which describes the size of wave function b [4].

$$\left(\frac{2\hbar}{m\omega_z}\right)^{1/2} = 2.1872 \times 10^{-3}\ m. \tag{5.6}$$

The length of the condensate in z direction is very small compared with the length in ρ direction. The huge ratio, ~ 375 that makes the condensate like a thread shape. We also calculate the peak condensate density, the maximum density at the center of the trap ($\rho = 0, z = 0$). the result is

$$\begin{aligned} |\phi(r)|^2 &= N\left(\frac{m\omega_\rho}{\pi\hbar}\right)\left(\frac{m\omega_z}{\pi\hbar}\right)^{1/2} \\ &= 8.2130 \times 10^{15}\ cm^{-3}. \end{aligned} \tag{5.7}$$

We can reanalyse the same situation using the Thomus-Fermi approximatiom.

In Chapter 3 we have calculated the ground state energy by using the measured the chemical potential through the peak density at the center of the condensate. In the Thomas-Fermi approximation, we obtain

$$\begin{aligned} E_o &= \frac{5}{7}N\mu(N) \\ &= 2.2490 \times 10^{-20} J. \end{aligned} \tag{5.8}$$

According to the Thomas-Fermi approximation, the density to vanishes at the edge of the condensate.

$$n_{cond}U_0 = \mu - V_{IP}(\rho, z) = 0 \tag{5.9}$$

Hence, we can calculate the size of the condensate cloud and obtain

$$\begin{aligned} \rho_{\max} &= \frac{1}{\alpha}\sqrt{\mu^2 + 2\mu\theta} = 7.3\ \mu m, \\ z_{\max} &= \sqrt{\frac{\mu}{\beta}} = 2.8\ mm. \end{aligned} \tag{5.10}$$

We find that the ground state energy is in good agreement with the experimental results.We can continue the calculation of energy in other trap shapes by the path integral theory and compare to those obtained from the Thomas-Fermi approximation. The results are sumarized in table(5.1).

5.2 The Wave Functions

We have calculated the ground wave function in Chapter 4. In this section, we study properties its physical implication. Recall that the ground wave function for one particle is

$$\begin{aligned} \phi_0(r) &= \left(\frac{m}{\pi\hbar}\left(\frac{\omega_\rho}{2} + \frac{\alpha^2\omega_z}{\omega_\rho(\gamma\hbar + 2m\omega_z\theta)} + \frac{(N-1)}{2}a\sqrt{\frac{m}{2\pi\hbar}}\omega_\rho\sqrt{\omega_z}\right)\right)^{1/2} \\ &\times \left(\frac{m}{\pi\hbar}\left(\frac{\omega_z}{2} + \frac{\gamma}{m\omega_z} + \frac{(N-1)}{2}a\sqrt{\frac{m}{2\pi\hbar}}\omega_\rho\sqrt{\omega_z}\right)\right)^{1/4} \\ &\times \exp\left[-\frac{m}{2\hbar}\left(\begin{array}{c}\left(\frac{\omega_\rho}{2} + \frac{\alpha^2\omega_z}{\omega_\rho(\gamma\hbar+2m\omega_z\theta)} + \frac{(N-1)}{2}a\sqrt{\frac{m}{2\pi\hbar}}\omega_\rho\sqrt{\omega_z}\right)\rho^2 \\ + \left(\frac{\omega_z}{2} + \frac{\gamma}{m\omega_z} + \frac{(N-1)}{2}a\sqrt{\frac{m}{2\pi\hbar}}\omega_\rho\sqrt{\omega_z}\right)z^2\end{array}\right)\right] \end{aligned} \tag{5.11}$$

Parameter	trap A		trap B	
$\alpha/k_B(\mu\mathrm{K/cm})$	15.9		9.5	
$\gamma/k_B(\mu\mathrm{K/cm}^2)$	25		25	
$\theta/k_B(\mu\mathrm{K})$	35±2		34±2	
	χ_c=χ_m	χ_c=$\chi_m/2$	χ_c=χ_m	χ_c=$\chi_m/2$
$\mu/k_B(\mu\mathrm{K})$	1.9	3.8	1.3	2.6
$\mathrm{N}_c(\times 10^9)$	1.2±0.2	6.6±1.3	1.2±0.1	6.7±0.5
Minimized parameter $\omega_\rho(\times 10^3\mathrm{Hz})$	3.79	1.94	2.08	1.01
Minimized parameter $\omega_z(\times 10^{-2}\mathrm{Hz})$	2.69	1.35	4.00	2.00
$\mathrm{n}_p(\times 10^{15}\mathrm{cm}^{-3})$ (Experiment)	4.8±0.4±1	9.7±0.7±2	3.3±0.1±0.7	6.5±0.2±1.3
$\mathrm{n}_p(\times 10^{15}\mathrm{cm}^{-3})$ (Theory)	8.2	16	5.5	11
Length $2\rho_{\max}(\mu\mathrm{m})$ (Experiment)	15	21	20	28
Length $2\rho_{\max}(\mu\mathrm{m})$ (Theory)	12	16	16	22
Length $2\mathrm{z}_{\max}$(mm) (Experiment)	5.5	7.8	4.5	6.4
Length $2\mathrm{z}_{\max}$(mm) (Theory)	4. 4	6.2	3.6	5.1
Total energy (J) (Experiment)	2.25×10^{-20}	2.47×10^{-19}	1.54×10^{-20}	1.67×10^{-19}
Total energy (J) (Theory)	2.47×10^{-20}	2.66×10^{-19}	1.65×10^{-20}	1.82×10^{-19}

Table 5.3: Summary of parameter describing the two trap shapes used for achieving BEC and comparing the result from the experiments to theory.

This ground state wave function solved by the path integral theory is of the same form as the wave function in Eq. (5.5) has different values ω_ρ and ω. Let

$$\psi_0(r) = \frac{\phi_0(r)}{\left[\begin{array}{c}\left(\frac{m\omega_\rho}{2\pi\hbar}\left(1+\frac{2\alpha^2\omega_z}{\omega_\rho^2(\gamma\hbar+2mb\theta)}+(N-1)a\sqrt{\frac{m}{2\pi\hbar}}\sqrt{\omega_z}\right)\right)^{1/2} \\ \times\left(\frac{m\omega_z}{\pi\hbar}\left(1+\frac{2\gamma}{m\omega_z^2}+(N-1)a\sqrt{\frac{m}{2\pi\hbar}}\frac{\omega_\rho}{\sqrt{\omega_z}}\right)\right)^{1/4}\end{array}\right]} \tag{5.12}$$

and

$$\begin{aligned} P^2 &= \frac{m\omega_\rho}{4\hbar}\rho^2 \\ Z^2 &= \frac{m\omega_\rho}{4\hbar}z^2, \end{aligned} \tag{5.13}$$

Then

$$\psi_0(r) = \exp-\left(\begin{array}{c}\left(1+\frac{2\alpha^2\omega_z}{\omega_\rho^2(\gamma\hbar+2mb\theta)}+(N-1)a\sqrt{\frac{m}{2\pi\hbar}}\sqrt{\omega_z}\right)P^2 \\ +\left(1+\frac{2\gamma}{m\omega_z^2}+(N-1)a\sqrt{\frac{m}{2\pi\hbar}}\frac{\omega_\rho}{\sqrt{\omega_z}}\right)Z^2\end{array}\right). \tag{5.14}$$

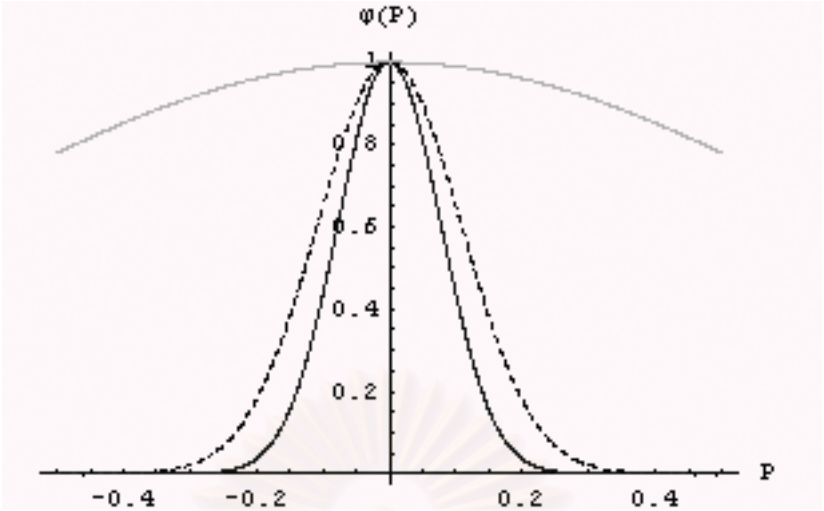

Figure 5.17: The behavior of wave function plotted against P. The solid line represent the $\psi_0(P)$ wave function. The dashed line is the non-interaction wave function and the light solid line is harmonic oscillator wave function.

Consider the P part of $\psi_0(r)$, call it $\psi_0(P)$,

$$\psi_0(P) = \exp\left[-\left(1 + \frac{2\alpha^2\omega_z}{\omega_\rho^2\left(\gamma\hbar + 2mb\theta\right)} + (N-1)a\sqrt{\frac{m}{2\pi\hbar}}\sqrt{\omega_z}\right)P^2\right] \qquad (5.15)$$

We now study behavior of $\psi_0(P)$ as a function P. The graphs from Figure 5.5 is a composite of the data from the trap shape A. The solid line is the function $\psi_0(P)$, which is of Gaussian shape. The dashed line represents the non-interaction wave function with the mean field interaction energy, $(N-1)a\sqrt{\frac{m}{2\pi\hbar}}\sqrt{\omega_z}$ excluded and the light solid line is $\psi_0(P) = e^{-P^2}$. We find that the harmonic oscillator wave function is very broad and $\psi_0(P)$ is shrunk vertically by the magnetic trap and the mean field interaction energy. Next, consider the Z part of $\psi_0(r)$, denoted by $\psi_0(Z)$,

$$\psi_0(Z) = \exp\left[-\left(1 + \frac{2\gamma}{m\omega_z^2} + (N-1)a\sqrt{\frac{m}{2\pi\hbar}}\frac{\omega_\rho}{\sqrt{\omega_z}}\right)Z^2\right].$$

The result for this case is similar to that of $\psi_0(P)$. In Fig. 5.5, the plot of the

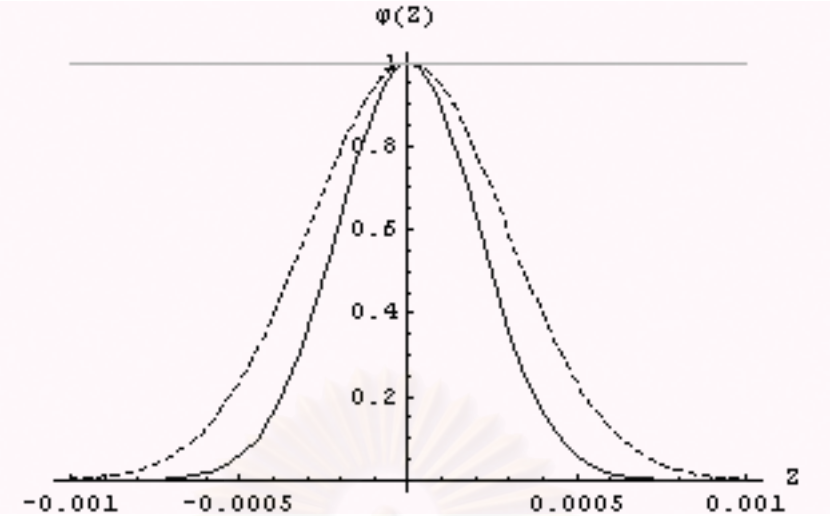

Figure 5.18: The behavior of wave function plotted against Z. The solid line is the $\psi_0(Z)$ wave function. The dashed line is non-interaction wave function and the light solid line is the harmonic oscillator wave function.

harmonic oscillator particle wave function in Z direction is very wide (as seen almost a straight line on the top) and $\psi_0(Z)$ has a narrow peak.

These behaviors of the ground state wave function can be interpreted physically. The very wide wave function of a harmonics oscillator implies that the probability of finding a particle is widely spread. When hydrogen atoms are confined by magnetic trap, the hydrogen atoms are confined in a very small area (about 5 mm$\times 10\mu$ m) and the probability of finding a particle becomes localized and has its maximum at the center of the trap.

สถาบันวิทยบริการ
จุฬาลงกรณ์มหาวิทยาลัย

Chapter 6
Conclusion

In this thesis, we have calculated the ground state energy and the wave function of Bose-Einstein condensation of atomic hydrogen by many-body Feynman path integral theory. We predicted and studied the behavior and the properties of hydrogen condensate such as the size of the condensate cloud, peak condensate density and the value of the ground state energy.

When Bose-Einstein condensation occurs, the macroscopic fraction of the hydrogen atoms occupy the lowest energy of about 10^{-20} J and have the same wave function. This wave function gives information about the size of the condensate and the density distribution. We found that many atoms occupy in a very small volume under the influence of a magnetic trap and interactions among the atoms, the diameter is $\sim$ 12 μm and the length is $\sim$ 5 mm. The peak density is $\sim 8 \times 10^{15}$ cm^{-3}, which is maximum at the center of the trap. However, hydrogen condensates are huge when compared with others alkali metal atoms. We also studied the influence of the interaction of the hydrogen condensate, It was found that the interaction energy of hydrogen atoms is very small and that it makes the hydrogens atom behave like an ideal Bose gas. Also the results from path integral theory are in good agreement with the Thomas-Fermi approximation.

The Calculation in Feynman path integral theory however is very complicated and very much differs from the simple Thomas-Fermi approximation. Nevertheless, Feynman path integral has advantages over the Thomas-Fermi approximation in that it is more realistic since we do not neglect the kinetic energy

term, although it is very small. The results are therefore more reliable. It is interesting to see if this method can be applied to the study of the properties of the excited states and other states of atomic hydrogen; it is our hope that this will be accomplished in the future

สถาบันวิทยบริการ
จุฬาลงกรณ์มหาวิทยาลัย

Reference

[1] R. P. Feynman. *Statistical Mechanics a Set of Lectures*. W. A. Benjamin., Massachusetts, 1972.

[2] D. G. Fried.*Bose-Einstein Condensation of Atomic Hydrogen*. Ph. D. thesis, Massachusetts Institute of Technology, 1999.

[3] D. G. Fried, T. C. Killian, L. Willmann, D. Landhuis, S. C. Moss, T. J. Greytak, and D. Kleppner. Bose-Einstein Condensation in Atomic Hydrogen. *Physica B*, 280: 20-26, 2000.

[4] R. P. Feynman and A. R. Hibbs. *Quantum Mechanics and Path Integrals*. McGraw-Hill, Singapore, international edition, 1995

[5] L.P. Pitaevskii, F. Dalfovo, S. Giorgini, and S. Stringari. Theory of Bose-Einstein condensation in trapped gases. *Rev. Mod. Phys.*, 71:463, 1998.

[6] C.J. Mayatt, M.J. Holland, E.A. Cornell, E.A. Burt, R.W. Ghrist, and C.E. Wieman. Coherence, correlations and collisions: What one learns about Bose-Einstein condensates from their decay. *Phys. Rev. Lett.*, 79:337, 1997.

[7] J.J. Tollet and C.C. Bradley C.A. Sackett and R.G. Hulet. Evidence condensation of bose-Einstein condensation in an Atomic Gas with Attractive Interactions. *Phys. Rev. Lett.*, 75:1687, 1995.

[8] N.J. van Druten, D.M. Kurn, D.S. Durfee, M.-O. Mewes, M.R. Andrews and W. Ketterle. Bose-Einstein condensation in a tightly confining dc magnetic trap. *Phys. Rev. Lett.*, 77:416, 1996.

[9] K.Huang. *Statistical Mechanics*. John Wiley and son, New York, 2nd edition.

1989.

[10] P. Ehrenfest and J.R Oppenheimer. Note on the statistics of nuclei. *Phys. Rev. Lett.*, 37:333, 1931.

[11] A. Dalgarno, M.J. Jamieson, and M. Kimura. Scattering lengths and effective ranges for He-He and spin-polarized H-H and D-D scattering. *Phys. Rev. A*,51:2626, 1995.

[12] W.C. Stwalley and L.H. Nosanow. Possible "new" quantum systems. *Phys. Rev. Lett.*, 36:910, 1976.

[13] T. C. Killian, D. G. Fried, L. Willmann, D. Landhuis, S. C. Moss, D. Kleppner, and T. J. Greytak. Bose-Einstein Condensation of Atomic Hydrogen. In *the International School of Physics Course*, 140, 1998

[14] T. C. Killian, A. D. Polcyn, J. C. Sandberg, I. A. Yu, T. J. Greytak, D. Kleppner, C. L. Cesar, D. G. Fried. Two-Photon Spectroscopy of Traped Atomic Hydrogen. *Phys. Rev. Lett.*, 77:255, 1996.

[15] B. Gross, J. Reichert, M. Prevedelli, M. Weitz, T. Udem, A. Huber, and T.W. Hansch. Phase-coherent measurement of the hydrogen 1S-2S transition frequency with an optical frequency interval divider chain. *Phys. Rev. Lett.*, 79:2646, 1997.

[16] T.C. Killian. *1S-2S Spectroscopy of Trapped Hydrogen. Ph.D. thesis, Massachusetts Institute of Technology*, 1999.

[17] L. Willmann, D. Landhuis, S. C. Moss, T. J. Greytak, D. Kleppner, T. C. Killian, and D. G. Fried. Cold Collision Frequency Shift of the 1S-2S Transition in Hydrogen. *Phys. Rev. Lett.*, 81:3807 1998.

[18] J.C. Sandberg. *Research Toward Laser Spectroscopy of Trapped Atomic Hy*

drogen. Massachusetts Institute of Technology, 1993.

[19] I.A. Yu, C.L. Cesar, D. Kleppner, J.M. Doyle, J.C. Sandberg, and T.W. Hijmans. Hydrogen in the submillikelvin regrim: stricking probability on superfluid He. *Phys. Rev. Lett.*, 67:603, 1991.

[20] M. Weidemuller, M.W. Reynolds, P.W.H. Pinkse, A. Mosk, and T.W. Hijmans. One-dimension evaporative cooling of magnetically trapped atomic hydrogen. *Phys. Rev. A*, 57:4747, 1998.

[21] E.D. Pritchard. Collisionless motion and evaporative cooling of atoms in a trap from precision spectroscopy. *Phys. Rev. Lett.*, 51:1336, 1983.

[22] J.T.M. Walraven, E.L. Surkov, and G.V Shlyapnikov. Collisionless motion and evaporative cooling of atoms in magnetic traps. *Phys. Rev. A*, 53:3403, 1996.

[23] G. Baym and C. J. Pethick. Ground-State Properties of Magnetically Trapped Bose-Condensed Rubidium Gas. *Phys. Rev. Lett.*, 76:6-9, 1996.

สถาบันวิทยบริการ
จุฬาลงกรณ์มหาวิทยาลัย

Appendix

สถาบันวิทยบริการ
จุฬาลงกรณ์มหาวิทยาลัย

Minimization of the ground state energy

In Chapter 5, we minimize the ground state energy by a Mathematica program as shown below.

$n = 1.2 \times 10^{9}; \hbar = 1.0546 \times 10^{-34}; k = 1.381 \times 10^{-29}; \alpha = 15.9 \times 10^{5} \times k;$

$m = 1.6746 \times 10^{-27}; a = 0.648 \times 10^{-10}; \gamma = 25 \times 10^{4} \times k; \theta = 35 \times k;$

$H = \frac{1}{2}\omega_\rho + \frac{1}{4}\omega_z + \frac{\gamma}{2\omega_z m} + \frac{\alpha^2 \omega_z}{\omega_\rho(\hbar\gamma + 2m\omega_z\theta)} + aN\sqrt{\frac{m}{2\pi\hbar}}\omega_\rho\sqrt{\omega_z};$

$\omega_\rho = \omega_\rho /.\text{NSolve}[\partial_{\omega_\rho} H == 0, \omega_\rho][[2]];$

$\text{FindMinimum}[H, \{\omega_z, 10^{-4}\}]$

$\%\hbar n$ (The result from minimization)

$\frac{5}{7}1.9nk$ (This is the calculation of energy from the experiment.)

Out[7]= {194987.,{0.0265919}}

Out[8]= $\{2.4671\times10^{-20}, \{1.26547 \times 10^{-25}(\omega_z \to 0.0265919)\}\}$

Out[9]= 2.24906×10^{-20}

In the 4^{th} line, we solve partial derivatives with respect to ω_ρ and select the second solution of which ω_ρ is positive. In the 5^{th} line, we find the minimum point by supposing the initial value of $\omega_z = 10^{-4}$ and multiply the result in the 5^{th} line by $\hbar n$ as shown in the 6^{th} line. We find that the ground state energy by the path integral theory is 2.4671×10^{-20} J and is 2.24906×10^{-20} for calculation from the experiment data.

ศูนย์วิทยทรัพยากร
จุฬาลงกรณ์มหาวิทยาลัย

Vitae

Mr. Wattana Lim was born on July 16, 1976 in Songkhla. He received his B.Sc. degree in physics from Prince of Songkhla University in 1988. During his study for a M.Sc. degree in physics at Chulalongkorn University, he research in theoretical physics. The topic of the research is Bose-Einstein condensation of atomic hydrogen with his supervisor Prof. Dr. Virulh Sa-yakanit.

สถาบันวิทยบริการ
จุฬาลงกรณ์มหาวิทยาลัย